Reciprocal influence between ranging codes and TC/TM

CCSDS Fall meeting, Darmstadt, November 2005
SLS-RNG_05-06

Giovanni Boscagli (ESA-ESTEC),
Enrico Vassallo (ESA-ESOC),
Monica Visintin (Politecnico di Torino)

1 Introduction

The paper analyzes the performance of the uplink and downlink transmission systems in the case of a regenerative PN ranging scheme. The error probabilities for the telecommand, telemetry and ranging systems are obtained through fast semianalytical measures, with either an ideal or a realistic transponder.

The RF system with the ideal transponder is simulated by adding the telecommand/telemetry signals and the ranging signal, passing them to an ideal phase modulator, which then feeds the receiver. Notice that this system is defined as baseband in [1].

The RF system with the realistic transponder is simulated

- in the uplink by adding the telecommand and ranging signals, and passing the resulting signal to an ideal phase modulator, as in the ideal case, but the receiver is preceded by the RX transponder filter;
- in the downlink by adding the telemetry and ranging signals, passing the resulting signal to an ideal phase modulator, the transponder TX filter and then the high power amplifier; the receiver is the same used for the ideal RF system (this case is labelled RF system in [1], where, however, a different filter model is used).

The simulated ranging signal chip rate is 2 Mchip/s; the uplink telecommand bit rate is 4 kbit/s, while the telemetry bit rate is 500 kbit/s. Thus one telecommand bit exactly corresponds to 8000 chips, while one telemetry bit exactly corresponds to 4 chips; the telecommand/telemetry and ranging signals are synchronized (the transition from one telecommand/telemetry bit to the subsequent one occurs at the same time of a transition from one chip to the following one). A different hypothesis is considered in [1] for the downlink, since the chip rate is 1.9 Mchip/s instead of 2 Mchip/s (one telemetry bit corresponds to 3.8 chips, 5 telemetry bits correspond to exactly 19 chips). The synchronization assumption probably leads to worst case results.

Two shaping pulses are considered for the ranging signal: the square and the half sine pulses.

Regarding the downlink, the following results have been obtained for the telemetry system:

- Considering the telemetry system losses due to the ranging signal as the parameter to be minimized, then the half sine pulse is more convenient for an ideal transponder, but the square pulse becomes more convenient when a realistic transponder is considered. This result is confirmed by the analysis in [1], even if a different filter is considered. If the

bandwidth occupancy alone in considered as the parameter to be minimized, then the half sine pulse becomes more convenient. If on-board complexity alone has to be minimized, then the square pulse becomes again the best choice. Thus no clear result can be given about the pulse to be used.

- Considering the telemetry system losses due to the ranging signal as the parameter to be minimized, then
  - For the ideal transponder, Tausworthe codes T2 and T2B show the worst performance (in accordance to [1]), Stiffler code SS6 has intermediate losses (but see the comments on the Stiffler codes below), while the other codes are almost equivalent; in absolute, the best results are obtained with codes S8, SS8 and T4B (in accordance to [1]).
  - For the realistic transponder, the codes have practically the same losses (about 0.1 dB of difference among the various codes), apart from codes T2, T2B and SS6 which confirm the higher losses obtained for the ideal transponder. The loss due to the presence of the TX filter and TWT amplifier can be estimated in the nearby of 0.35 dB; in [1] a larger loss is measured, but the TX filter is different; the analysis in [1], regarding only codes JPL99, T4B, SS8, confirm that the difference among the codes in terms of telemetry loss is very small.

- The Stiffler ranging codes (both scrambled and unscrambled) have a component that is generated by a square wave with period equal to 4 chips; within the 4 chips, this ranging code component is exactly equal to one telemetry pulse (SP-L). Therefore there is a strong influence between the Stiffler ranging signal and the telemetry signal. Notice that this phenomenon occurs for the chosen telemetry bit rate and ranging chip rate, while it is not present for the rate values chosen in [1]. The effects of this correspondence between a component of the ranging signal and the telemetry signal is that the telemetry bit error rate actually depends on the transmitted telemetry bits, especially at high signal to noise ratios. Tausworthe codes does not show this problem, since they are built from sequences having periodicity $L_i T_c$ with L_i prime number. Notice that a telemetry bit rate equal to 1 Mbit/s would produce a strong interference with the clock component of the ranging signal (also the Tausworth codes would be affected by this problem).

Regarding the downlink, the following results have been obtained for the ranging system:

- Considering the ranging system losses due to the telemetry signal as the parameter to be minimized, then the square pulse is more convenient for both the ideal and the realistic transponder.

- The performance of the Stiffler codes highly depends on the telemetry bit sequence, especially for the decision on the phase of the square wave probing signal of periodicity equal to 4 chips. In certain cases, the detected ranging signal phase can be wrong even in the absence of noise, however, a very good sequence of telemetry bits (which was considered in the simulations) leads to practically no losses for codes S6 and S8.

- Among the Tausworthe codes, the minimum losses are experienced by codes T2 and T2B.

- The minimum ranging phase acquisition times are obtained by codes T2/T2B, followed by codes S6/SS6, codes T4/T4B, codes S8/SS8 and finally code JPL99. The strongest clock component that allows for easier clock acquisition is found in code JPL99, followed by codes S8/SS8 and T4/T4B (very similar), codes S6/SS6 and then codes T2/T2B.

Regarding the uplink, it is shown that the telecommand losses due to the interfering ranging signals are very small for the chosen modulation indexes, and no significant difference exists between the two considered shaping pulses. The square pulse is more convenient when considering the losses of the ranging system; only code S6 seems to suffer from a relative large loss (0.45 dB) caused by the interfering telecommand signal, while the other codes are all equivalent.

Based on the above results, which however need to be extended and further analyzed, the best choice for the ranging code seems to be code T4 or T4B.

2 System description

2.1 Ground station transmitter

The transmitted signal in the uplink is (see fig. 1)

$$x_u(t) = A_c \cos[2\pi F_u t + m_{RG} x_{RG}(t) + m_{TC} x_{TC}(t)] \tag{1}$$

where

- F_u is the uplink center frequency
- m_{RG} is the phase modulation index for the ranging signal ($m_{RG} = 0.7$ in the simulations);
- m_{TC} is the phase modulation index for the telecommand signal ($m_{TC} = 1$ in the simulations);
- $x_{RG}(t)$ is the ranging signal:

$$x_{RG}(t) = \sum_{k=-\infty}^{\infty} c_k h(t - kT_{RG}) \tag{2}$$

  and $h(t)$ is different from zero only for $t \in [0, T_{RG}]$, and may be either a rectangular pulse ($h(t) = h_{sq}(t)$) or a half cycle sine ($h(t) = h_{sin}(t) = \sin(\pi t/T_{RG})$), $T_{RG} = 1/R_c$ is the chip interval and R_c is the chip rate (2 Mchip/s in the simulations), $c_k = \pm 1$ is the periodic sequence of values determined by the chosen ranging code;

- $x_{TC}(t)$ is the telecommand signal:

$$x_{TC}(t) = \sum_{k=-\infty}^{\infty} d_k g_{TC}(t - kT_{TC}) \tag{3}$$

  and $g_{TC}(t) = \sin(2\pi f_s t)$ for $t \in [0, T_{TC}]$, and zero elsewhere, $T_{TC} = 1/R_{TC}$ is the telecommand bit interval and R_{TC} is the bit rate for the telecommand data ($R_{TC} = 4$ kbit/s and $f_s = 16$ kHz in the simulations), $d_k = \pm 1$ is a random sequence; in the following, the auxiliary signal $u_{TC}(t) = 1$ for $t \in [0, T_{TC}]$ and zero elsewhere will be used;

The total energies used to carry one ranging chip and one telecommand bit are, respectively,

$$E_{RG} = \begin{cases} \frac{A_c^2}{2} \frac{1+J_0(2m_{TC})}{2} \sin^2[m_{RG}] T_{RG} & h(t) = h_{sq}(t) \\ \frac{A_c^2}{2} \frac{1+J_0(2m_{TC})}{2} \frac{1-J_0(2m_{RG})}{2} T_{RG} & h(t) = h_{sin}(t) \end{cases} \tag{4}$$

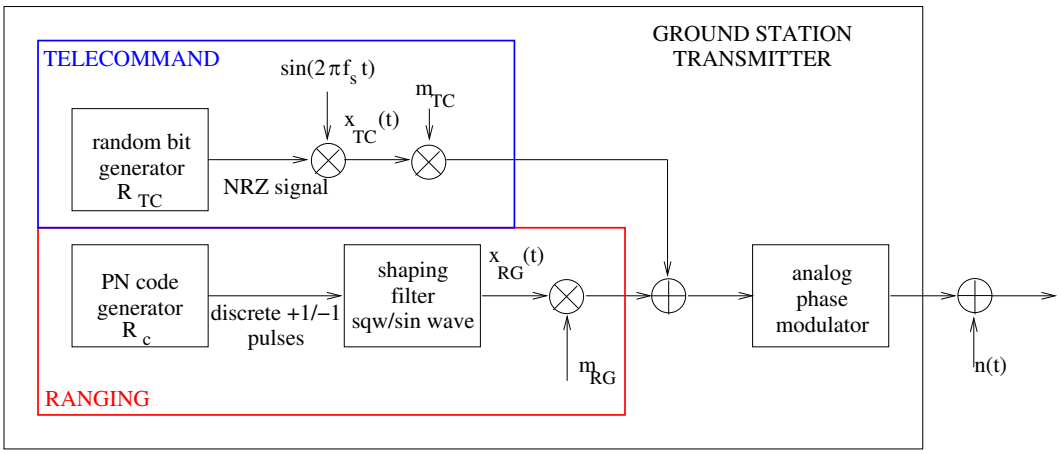

Figure 1: Block diagram of the ground station transmitter.

$$E_{TC} = \begin{cases} \frac{A_c^2}{2}\cos^2[m_{RG}]\frac{1-J_0(2m_{TC})}{2}T_{TC} & h(t) = h_{sq}(t) \\ \frac{A_c^2}{2}\frac{1+J_0(2m_{RG})}{2}\frac{1-J_0(2m_{TC})}{2}T_{TC} & h(t) = h_{sin}(t) \end{cases} \tag{5}$$

In general, however, the receiver useful energies are considered, which are

$$E_{RG,u} = \begin{cases} \frac{A_c^2}{2}J_0^2(m_{TC})\sin^2(m_{RG})T_{RG} & h(t) = h_{sq}(t) \\ \frac{A_c^2}{2}2J_0^2(m_{TC})J_1^2(m_{RG})T_{RG} & h(t) = h_{sin}(t) \end{cases} \tag{6}$$

$$E_{TC,u} = \begin{cases} \frac{A_c^2}{2}\cos^2(m_{RG})2J_1^2(m_{TC})T_{TC} & h(t) = h_{sq}(t) \\ \frac{A_c^2}{2}2J_1^2(m_{TC})J_0^2(m_{RG})T_{TC} & h(t) = h_{sin}(t) \end{cases} \tag{7}$$

Which of the two definitions of energies should be used depend on the receiver structure: the ideal receiver that works on the complete received signal must be analyzed referring to eqns. (4) and (5), while the more common receiver that uses only the main component must be analyzed referring to eqns. (6) and (7). This topic shall be treated again when describing the receiver structures.

2.2 Satellite transmitter

The transmitted signal in the downlink is (see fig. 2)

$$x_d(t) = A_c\cos[2\pi F_d t + m_{RG}x_{RG}(t) + m_{TM}x_{TM}(t)] \tag{8}$$

where

- F_d is the downlink center frequency;
- m_{RG} is the phase modulation index for the ranging signal ($m_{RG} = 0.7, 0.5, 0.2$ in the simulations);
- m_{TM} is the phase modulation index for the telemetry signal ($m_{TM} = 1.25$ in the simulations);

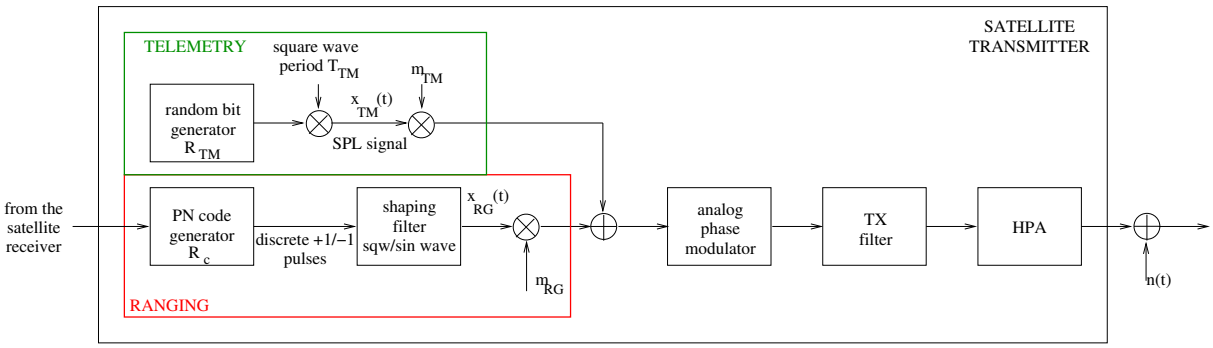

Figure 2: Block diagram of the satellite transmitter.

- $x_{RG}(t)$ is the ranging signal:

$$x_{RG}(t) = \sum_{k=-\infty}^{\infty} c_k h(t - kT_{RG}) \tag{9}$$

  and $h(t) = h_{sq}(t)$ or $h(t) = h_{sin}(t)$ as for the uplink;

- $x_{TM}(t)$ is the telemetry signal:

$$x_{TM}(t) = \sum_{k=-\infty}^{\infty} d_k p_{TM}(t - kT_{TM}) \tag{10}$$

  and $p_{TM}(t) = 1$ for $t \in [0, T_{TM}/2]$, $p(t) = -1$ for $t \in [T_{TM}/2, T_{TM}]$, $T_{TM} = 1/R_{TM}$ is the telemetry bit interval and R_{TM} is the bit rate for the telemetry data ($R_{TM} = 500$ kbit/s in the simulations), $d_k = \pm 1$ is a random sequence;

- the total transmitted power is $P_T = A_c^2/2$, only a part of which is used for the telemetry signal and for the ranging signal.

The total energies used to carry one ranging chip and one telemetry bit are, respectively,

$$E_{RG} = \begin{cases} \frac{A_c^2}{2} \cos^2[m_{TM}] \sin^2[m_{RG}] T_{RG} & h(t) = h_{sq}(t) \\ \frac{A_c^2}{2} \cos^2[m_{TM}] \frac{1 - J_0(2m_{RG})}{2} T_{RG} & h(t) = h_{sin}(t) \end{cases} \tag{11}$$

$$E_{TM} = \begin{cases} \frac{A_c^2}{2} \cos^2[m_{RG}] \sin^2[m_{TM}] T_{TM} & h(t) = h_{sq}(t) \\ \frac{A_c^2}{2} \frac{1 + J_0(2m_{RG})}{2} \sin^2[m_{TM}] T_{TM} & h(t) = h_{sin}(t) \end{cases} \tag{12}$$

The receiver useful energies are

$$E_{RG} = \begin{cases} \frac{A_c^2}{2} \cos^2[m_{TM}] \sin^2[m_{RG}] T_{RG} & h(t) = h_{sq}(t) \\ \frac{A_c^2}{2} \cos^2[m_{TM}] 2J_1^2(2m_{RG}) T_{RG} & h(t) = h_{sin}(t) \end{cases} \tag{13}$$

$$E_{TM} = \begin{cases} \frac{A_c^2}{2} \cos^2[m_{RG}] \sin^2[m_{TM}] T_{TM} & h(t) = h_{sq}(t) \\ \frac{A_c^2}{2} J_0^2(m_{RG}) \sin^2[m_{TM}] T_{TM} & h(t) = h_{sin}(t) \end{cases} \tag{14}$$

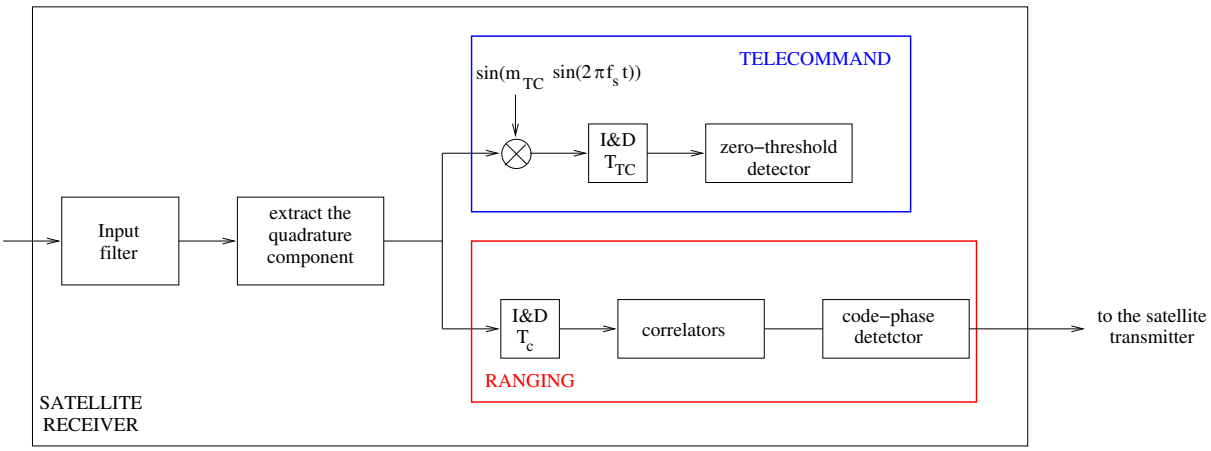

Figure 3: Block diagram of the satellite receiver.

As described in the previous section, eqns. (11) and (12) must be used for the ideal receiver that uses all the components of the transmitted signal, while eqns. (13) and (14) should be used for the more common receiver that uses only the main component.

2.3 Considered ranging codes

The following pseudo-noise (PN) ranging codes are considered in the analysis:

- JPL-99 code (labelled as JPL99, and used as reference),
- in the Tausworthe family:
  1. Tausworthe code with clock vote $v = 2$ (labelled as T2),
  2. Tausworthe code with clock vote $v = 4$ (labelled as T4),
  3. balanced Tausworthe code with clock vote $v = 2$ (labelled as T2B),
  4. balanced Tausworthe code with clock vote $v = 4$ (labelled as T4B),
- in the Stiffler family:
  1. Stiffler code with clock vote $v = 6$ (labelled as S6),
  2. Stiffler code with clock vote $v = 8$ (labelled as S8),
  3. scrambled Stiffler code with clock vote $v = 6$ (labelled as SS6),
  4. scrambled Stiffler code with clock vote $v = 8$ (labelled as SS8).

2.4 Satellite telecommand receiver

Figure 3 shows the block diagram of the satellite receiver. The telecommand receiver is made of a filter matched to the waveform

$$p(t) = \sin[m_{TC} \sin(2\pi f_s t)] u_{TC}(t) \tag{15}$$

followed by a sampler and a zero-threshold detector.

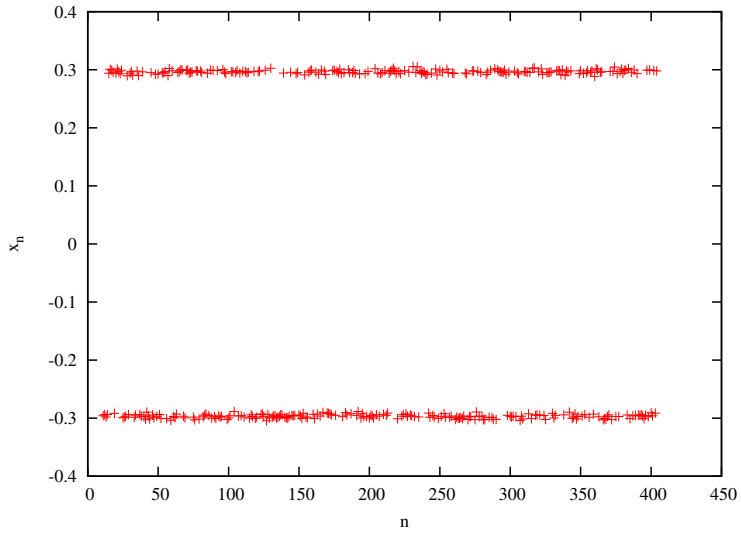

Figure 4: Input x_n of the telecommand zero-threshold detector in the case of ideal transponder, $h(t) = h_{sq}(t)$, $m_{TC} = 1$, $m_{RG} = 0.7$, no noise. The interference of the ranging signal can be seen as small fluctuations around the ideal values ± 0.3.

2.4.1 Case of $h(t) = h_{sq}(t)$

In the case of $h(t) = h_{sq}(t)$, the telecommand receiver is ideal and, assuming no interference from the ranging signal, the error probability for the telecommand bit is

$$P_{id,TC}(e) = \frac{1}{2}\,\mathrm{erfc}\,\sqrt{\frac{E_{TC}}{N_0}}, \tag{16}$$

i.e. the error probability of an ideal 2-PAM system. The presence of the interfering ranging signal introduces a loss which may be different from code to code and which must be evaluated through the simulation. Fig. 4 shows the samples x_n at the input of the detector in the presence of the ranging signal, but in the absence of noise. It can be noticed that the amount of interference is very small and the losses due to the ranging signals can be expected to be very small. Notice that the ranging signal alone never generates such a high interference to cause an error in the telecommand system; therefore no error floor is present for the telecommand bits.

Notice that more common telecommand receivers multiply the incoming signal by $\sin(2\pi f_s t)$ (instead of $\sin[m_{TC}\sin(2\pi f_s t)]$): in this case the error probability in the absence of interference from the ranging signal is

$$\begin{aligned} P_{id,TC}(e) &= \frac{1}{2}\,\mathrm{erfc}\,\frac{A_c\cos(m_{RG})T_{TC}J_1(m_{TC})}{\sqrt{N_0 T_{TC}}} \\ &= \frac{1}{2}\,\mathrm{erfc}\,\sqrt{\frac{E_{TC,u}}{N_0}}, \end{aligned} \tag{17}$$

which justifies the use of the useful receiver energy $E_{TC,u}$ instead of E_{TC}. Since in our analysis the ideal receiver is considered, we shall use E_{TC}; the study will be expanded in the future in order to consider the more common telecommand receiver. The loss of the common receiver with respect to the ideal one is negligible, since it amounts to $10\log_{10} E_{TC}/E_{TC,u} = 0.008$ dB for $m_{TC} = 1$ and $m_{RG} = 0.7$.

2.4.2 Case of $h(t) = h_{sin}(t)$

In the case of $h(t) = h_{sin}(t)$, the telecommand receiver is not ideal (the filter should be matched to $p(t) = \cos[m_{RG}|\sin(\pi t/T_{RG})|]\sin[m_{TC}\sin(2\pi f_s t)]u_{TC}(t)$), and a loss is present even in the absence of the interfering ranging signal. It can be shown that

$$P_{id,TC}(e) = \frac{1}{2}\,\mathrm{erfc}\,\sqrt{\frac{E_{TC}}{N_0}\frac{J_0^2[m_{RG}]}{[1+J_0(2m_{RG})]/2}} \tag{18}$$

The loss in decibel is

$$\text{Loss } = 10\log_{10}\frac{[1+J_0(2m_{RG})]/2}{J_0^2[m_{RG}]} \tag{19}$$

which amounts to 0.0385 dB for $m_{RG} = 0.7$ Therefore, even if the telecommand receiver is not ideal, it is simpler and the loss is almost negligible.

The more common telecommand receiver would produce

$$\begin{aligned} P_{id,TC}(e) &= \frac{1}{2}\,\mathrm{erfc}\,\frac{A_c J_0(M_{RG})J_1(m_{TC})T_{TC}}{\sqrt{N_0 T_{TC}}} \\ &= \frac{1}{2}\,\mathrm{erfc}\,\sqrt{\frac{E_{TC,u}}{N_0}}. \end{aligned} \tag{20}$$

Thus, if we use $E_{TC,u}$ as definition of energy, the system introduces no losses with respect to the ideal 2-PAM system. However, with respect to the total transmitted energy E_{TC}, it is possible to measure a loss which amounts to $10\log_{10} E_{TC}/E_{TC,u} = 0.05$ dB for $m_{RG} = 0.7$ and $m_{TC} = 1$. The more common telecommand receiver is thus practically optimum also in this case.

2.4.3 BER evaluation through semianalytical technique

The input of the zero-threshold detector in the telecommand receiver can be modelled as

$$y_n = \alpha d_n + \zeta_n + \nu_n = x_n + \nu_n \tag{21}$$

where d_n is the level corresponding to the transmitted telecommand bit, ζ_n is the interference due to the ranging signal and ν_n is the noise contribution. An example of the values of x_n is shown in figure 4.

The error probability for $\zeta_n \neq 0$ can be evaluated through a very fast semianalytical technique. The system is simulated in the absence of noise, so that the detector inputs are the samples $x_n = \alpha d_n + \zeta_n$. Assume that ζ_n is small with respect to α, so that the sign of $\alpha d_n + \zeta_n$ is the sign of d_n. Moreover, assume that $d_n = -1$, so that $x_n = -\alpha + \zeta_n$. If noise were present, the error probability would be

$$\begin{aligned} P_{TC}(e|d_n = -1, \zeta_n) &= P(\alpha d_n + \zeta_n + \nu_n > 0 | d_n = -1) \\ &= P(\nu_n > \alpha - \zeta_n) = \frac{1}{2}\,\mathrm{erfc}\,\frac{\alpha - \zeta_n}{\sqrt{2\sigma^2}} \\ &= \frac{1}{2}\,\mathrm{erfc}\,\frac{|x_n|}{\sqrt{2\sigma^2}}. \end{aligned} \tag{22}$$

Assume now that $d_n = 1$, so that $x_n = \alpha + \zeta_n$. If noise were present, the error probability would be

$$\begin{aligned} P_{TC}(e|d_n = 1, \zeta_n) &= P(\alpha d_n + \zeta_n + \nu_n < 0 | d_n = 1) \\ &= P(\nu_n < -\alpha - \zeta_n) = P(\nu_n > \alpha + \zeta_n) \\ &= \frac{1}{2}\,\mathrm{erfc}\,\frac{\alpha + \zeta_n}{\sqrt{2\sigma^2}} = \frac{1}{2}\,\mathrm{erfc}\,\frac{|x_n|}{\sqrt{2\sigma^2}}. \end{aligned} \tag{23}$$

Then, in general,

$$P_{TC}(e|x_n) = \frac{1}{2} \text{ erfc } \frac{|x_n|}{\sqrt{2\sigma^2}}. \tag{24}$$

Considering a simulation run in which N_{sym} telecommand bits are simulated, the average error probability may be evaluated as

$$P_{TC}(e) = \frac{1}{N_{sym}} \sum_{n=1}^{N_{sym}} P_{TC}(e|x_n) = \frac{1}{N_{sym}} \sum_{n=1}^{N_{sym}} \frac{1}{2} \text{ erfc } \frac{|x_n|}{\sqrt{2\sigma^2}}. \tag{25}$$

2.5 Satellite ranging receiver

The satellite ranging receiver shown in figure 3 is not optimum, but it is simple, as required on-board. With some simplifications, it can be shown that the losses in the absence of telecommand interference are approximately

$$\text{Loss }_{sq} \simeq 10 \log_{10} \frac{[1 + J_0(2m_{TC})]/2}{J_0^2[m_{TC}]} \tag{26}$$

for $h(t) = h_{sq}(t)$ and

$$\text{Loss }_{sin} \simeq 10 \log_{10} \frac{[1 + J_0(2m_{TC})]/2}{J_0^2[m_{TC}]} \frac{[1 - J_0(2m_{RG})]/2}{E_0^2[m_{RG}]} = \text{ Loss }_{sq} + \Delta_{Loss}(m_{RG}) \tag{27}$$

for $h(t) = h_{sin}(t)$. For $m_{TC} = 1$ and $m_{RG} = 0.7$, Loss $_{sq} = 0.191$ dB and Loss $_{sin} = 1.045$ dB. Notice that these losses are evaluated with respect to the total transmitted energy. when we consider the receiver useful energies, then we find no loss in the case $h(t) = h_{sq}(t)$, and 1 dB loss for $h(t) = h_{sin}(t)$, due to the mismatch between the transmitted sinusoidal pulse and the simple integrate and dump receiver.

2.5.1 Ranging performance, Tausworthe codes.

In a baseband transmission (i.e. assuming that the ranging signal alone is transmitted at baseband as an NRZ signal, without RF phase modulation and without the telecommand interference), the input of the ranging receiver is

$$r(t) = s_r(t) + n(t) \tag{28}$$

where $s_r(t)$ is the transmitted ranging signal and $n(t)$ is the additive noise (power spectrum $N_0/2$). The receiver evaluates the correlation coefficients

$$\lambda_{ik} = \int_0^{t_o} r(t) p_{ik}(t) dt = \int_0^{t_o} s_r(t) p_{ik}(t) dt + \int_0^{t_o} n(t) p_{ik}(t) dt = \rho_{ik} + \nu_{ik} \tag{29}$$

between the received signal and the various probing signals $p_{ik}(t) = p_i(t - (k-1)T_{RG})$, and for each i finds the maximum. It is possible to theoretically evaluate ρ_{ik} and the probability $P_i(C)$ that the detected phase of each of the 6 subcodes is correct: It can be shown that

$$P_1(C) = 1 - \frac{1}{2} \text{ erfc } \frac{\rho_{11}}{\sqrt{2}\sigma_1} \tag{30}$$

$$P_i(C) = \int_{-\infty}^{\infty} \left[\prod_{k=2}^{L_i} 1 - \frac{1}{2} \text{ erfc } \left(y - \frac{\rho_{ik} - \rho_{i1}}{\sqrt{2}\sigma_\nu} \right) \right] \frac{1}{\sqrt{\pi}} e^{-y^2} dy \tag{31}$$

$\tilde{\rho}_{ik}$	JPL99	T2	T2B	T4	T4B
$\tilde{\rho}_{11}$	963390	623400	633306	942600	947566
$\tilde{\rho}_{12}$	-963390	-623400	-633306	-942600	-947566
$\tilde{\rho}_{21}$	46080	261510	247020	66870	61904
$\tilde{\rho}_{2k},\ k = 2, \ldots, 7$	0	-26906	-41404	-6930	-10368
$\tilde{\rho}_{31}$	46080	259374	250404	66870	61904
$\tilde{\rho}_{3k},\ k = 2, \ldots, 11$	0	-15930	-24900	-4158	-6160
$\tilde{\rho}_{41}$	46080	257910	251332	66870	61904
$\tilde{\rho}_{4k},\ k = 2, \ldots, 15$	0	-11274	-17852	-2970	-4400
$\tilde{\rho}_{51}$	46080	256926	251604	66870	61904
$\tilde{\rho}_{5k},\ k = 2, \ldots, 19$	0	-8714	-14056	-2310	-3456
$\tilde{\rho}_{61}$	46080	256230	251940	66870	61904
$\tilde{\rho}_{6k},\ k = 2, \ldots, 23$	0	-7098	-11388	-1890	-2800

Table 1: Correlation coefficients $\tilde{\rho}_{ik}$ for the various Tausworthe ranging codes, observation interval $t_o = T_r = L_r T_c = 1009470 T_{RG}$.

where E_c is the energy used to transmit one chip, $\rho_{ik} = \tilde{\rho}_{ik}\sqrt{E_c T_{RG}}$ is given in table 1,

$$\sigma_1^2 = \frac{N_0}{2} T_r \tag{32}$$

and

$$\sigma_\nu^2 = \frac{N_0}{2}\left(1 + \frac{1}{L_i}\right) T_r \tag{33}$$

for the parallel receiver (77 correlators)[1], and

$$\sigma_\nu^2 = \frac{N_0}{2} T_r \tag{34}$$

for the completely serial receiver (6 correlators) for which the observation interval t_o is equal to the ranging signal period T_r.

The overall error probability in the detection of the ranging code phase is

$$P_{RG}(e) = 1 - \prod_{i=1}^{6} P_i(C) \tag{35}$$

The above equations for the error probability may be used also for the RF system, provided that the correct new values of ρ_{ik} are used. Being $x_{\Im,u}(t)$ the quadrature component of the received signal in the absence of noise, it is sufficient to measure through simulation the set of values

$$\rho'_{ik} = \int_0^{t_o} x_{\Im,u}(t) p_{ik}(t) dt = \sum_{n=1}^{L_r} c_{ik}(n) \int_{nT_{RG}}^{(n+1)T_{RG}} x_{\Im,u}(t) dt = \sum_{n=1}^{L_r} c_{ik}(n) x_n \tag{36}$$

where $c_{ik}(n)$ is the n-th chip of subcode C_i shifted by k steps, and x_n is the output of the integrate and dump filter shown in fig. 3, without noise. Then we use these new values ρ'_{ik} instead of those listed in table 1.

[1]Since the Tausworthe probing sequences are not orthogonal to their time-shifted versions, the parallel receiver suffers from a small loss due to the correlation among the noise terms; the serial receiver, on the contrary, observes subsequent portions of white noise and the noise terms are therefore statistically independent.

$\tilde{\rho}_i$	S6	SS6	S8	SS8
$\tilde{\rho}_1$	873392	873392	981920	981920
$\tilde{\rho}_i$, $i = 2, \ldots, 20$	74256	74256	34272	34272

Table 2: Values of $\tilde{\rho}_i$ for the considered Stiffler codes

2.5.2 Ranging performance, Stiffler codes

For the Stiffler codes the decision process is made of parallel/serial binary decisions, and it is possible to show that, in the case of baseband transmission, the probability of correct detection of the ranging code phase, assuming an observation interval $t_o = T_r = 2^{20} T_{RG}$ (the period of the ranging signal) is

$$P(C) = \prod_{i=1}^{20} \left(1 - \frac{1}{2} \operatorname{erfc} \sqrt{\frac{\rho_i^2}{N_0 T_r}} \right). \tag{37}$$

where

$$\rho_i = \int_0^{t_o} s_r(t) p_i(t) dt \tag{38}$$

being $p_i(t)$ the probing signal, i.e. a square wave with period $2^i T_{RG}$ and duty cycle equal to 0.5 (for the unscrambled Stiffler codes), and $s_r(t)$ the baseband ranging signal[2]. The values of $\tilde{\rho}_i = \rho_i / \sqrt{E_{RG} T_{RG}}$ are given in table 2.

For the RF transmission, it is simply sufficient to change ρ_i into ρ_i' in eqn. (37), where again

$$\rho_i' = \int_0^{t_o} x_{\Im,u}(t) p_i(t) dt, \tag{39}$$

can be measured through simulation.

2.6 Ground station receiver

Figures 5 and 6 show the block diagrams of the ground station receiver, for $h(t) = h_{sq}(t)$ and $h(t) = h_{sin}(t)$, respectively.

2.6.1 The telemetry system

The structure of fig. 5 relative to the case $h(t) = h_{sq}(t)$ is ideal, and the losses are only due to the reciprocal interference between the telemetry and ranging signals. In this case the total and useful energies are equal, and there is no ambiguity in the definition of the signal to noise ratio.

The ideal telemetry receiver with $h(t) = h_{sin}(t)$ (fig. 6) should multiply the input signal also by $\cos[m_{RG} |\sin(\pi t / T_{RG})|]$. The considered simplified receiver thus introduces the following loss

$$\text{Loss } = 10 \log_{10} \frac{[1 + J_0(2m_{RG})]/2}{J_0^2[m_{RG}]} \tag{40}$$

which amounts to 0.0385 dB for $m_{RG} = 0.7$, 0.0092 dB for $m_{RG} = 0.5$, 2.2×10^{-4} dB for $m_{RG} = 0.2$. The receiver of fig. 6 is thus practically ideal for the considered values of m_{RG}.

[2]For the Stiffler codes there is no difference in the performance of parallel and serial receivers, since the decisions are binary, and the probing signals are all orthogonal among each other

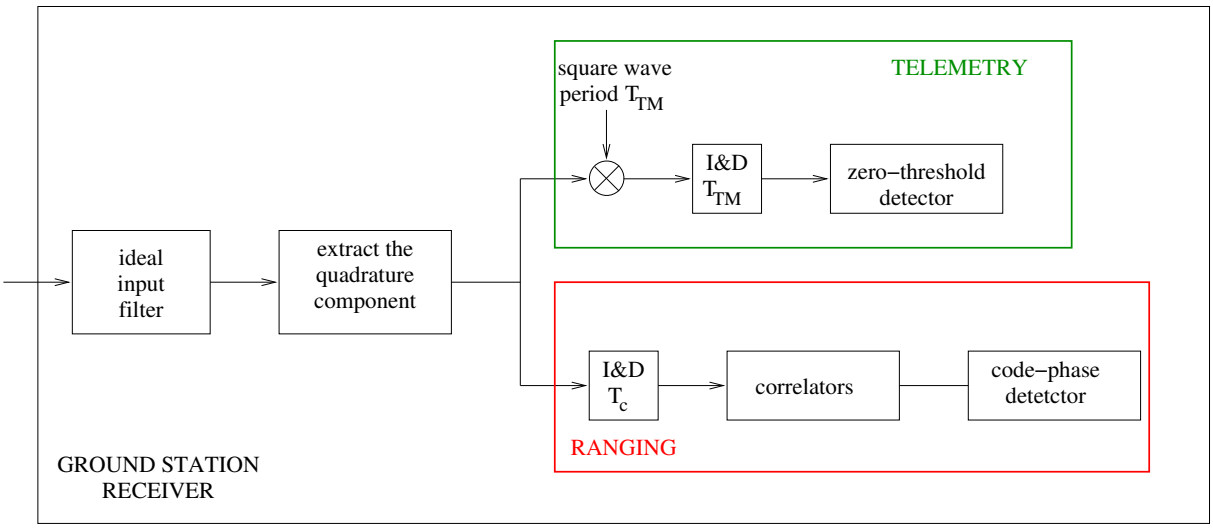

Figure 5: Block diagram of the ground station receiver (case of $h(t) = h_{sq}(t)$).

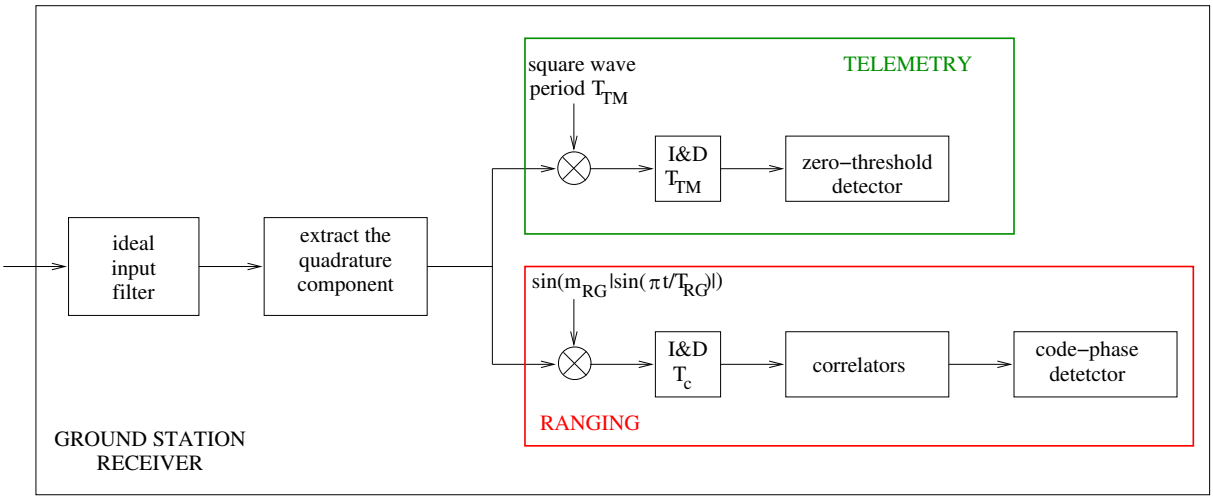

Figure 6: Block diagram of the ground station receiver (case of $h(t) = h_{sin}(t)$).

These losses are evaluated considering the total transmitted energy. If the useful transmitted energy were considered, no loss would be found. However, since the difference between E_{TM}/N_0 and $E_{TM,u}/N_0$ is at most 0.0385 dB, the two definitions of signal to noise ratios can be used equivalently for practical purposes.

The semianalytical techniques described for the uplink channel can be applied also in this case.

Figures 7–10 show the noisyless input of the telemetry zero-threshold detector in the case $h(t) = h_{sq}(t)$. The presence of interference due to the ranging code is evident: the inputs to the detector in the absence of the ranging signal are equal to ± 0.7, but the ranging signal introduces interference and, for the case of figure 7 the inputs take the values ± 0.6, ± 0.7 ± 0.8. It is possible to show that the interference ζ_n which affects x_n is

$$\zeta_n = A_c \cos(m_{TM}) \sin(m_{RG}) \int_{nT_{TM}}^{(n+1)T_{TM}} p_{TM}(t - nT_{TM}) \sum_k c_k h_{sq}(t - kT_{RG}). \tag{41}$$

which can take the values 0, $\pm A_c \cos(m_{TM}) \sin(m_{RG}) T_{TM}/2 = \pm a$ (where $a \simeq 0.1$ in the examples of figures 7–10), and $\pm 2a$. The value $2a$ occurs only if the 4 chips involved in the above integral are equal to $[1, 1, -1, -1]$, while the value a occurs for 4 the sequences $[1, 1, 1, -1]$, $[1, 1, -1, 1]$, $[1, -1, -1, -1]$, and $[-1, 1, -1, -1]$, etc. If the ranging sequence c_k were random, ζ_n would be equal to $2a$ with probability 1/16, to a with probability 1/4, to 0 with probability 6/16. Since the ranging codes are not random sequences, these probabilities change. From figures 7–10, it is possible to notice that code JPL99 never gives rise to $\zeta_n = \pm 2a$, codes S6 and S8 only generate $\zeta_n = a$, codes T2 and T2B generate $\zeta_n = \pm 2a$ with a higher probability than codes T4 and T4B, codes SS6 and SS8 give rise to $\zeta_n = \pm a$ or $-2a$. Based on these considerations, it can be expected that three subsets of codes are present: the subset made of JPL99, S6 and S8 will have the smaller error probabilities, followed by the subset containing codes T4 and T4B, while the subset with SS6, SS8, T2 and T2B will generate the higher error probabilities. Since the interference generated by the Stiffler codes is mostly positive, the telemetry system performance will depend on the fact that the transmitted telemetry level is positive (constructive interference) or negative (destructive interference). If, for example, the telemetry levels were all positive, then the measured error probability would be lower than that of the ideal 2PAM system (only constructive interference). As a consequence the measured error probabilities may vary by changing the statistical properties of the generated telemetry data, and the variations are not negligible, especially at high E_{TM}/N_0 values, which justifies the differences found with respect to [1]. The analysis of figures 7–10 in any case allows to state that the interference on the telemetry system due to the ranging signal produces an error probability $P_{TM} = 0$ in the absence of noise, and therefore no error floor exists.

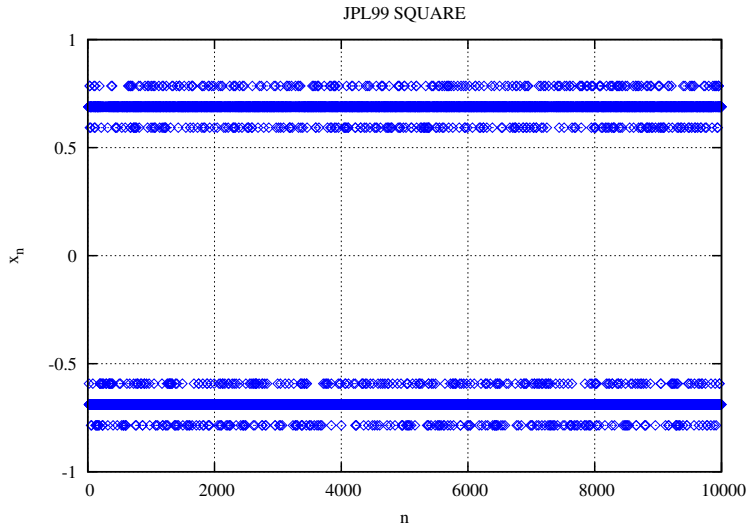

Figure 7: Samples x_n at the input of the zero threshold detector of the telemetry receiver. Case of code JPL99, $h(t) = h_{sq}(t)$; $m_{TM} = 1.25$ and $m_{RG} = 0.7$, ideal transponder.

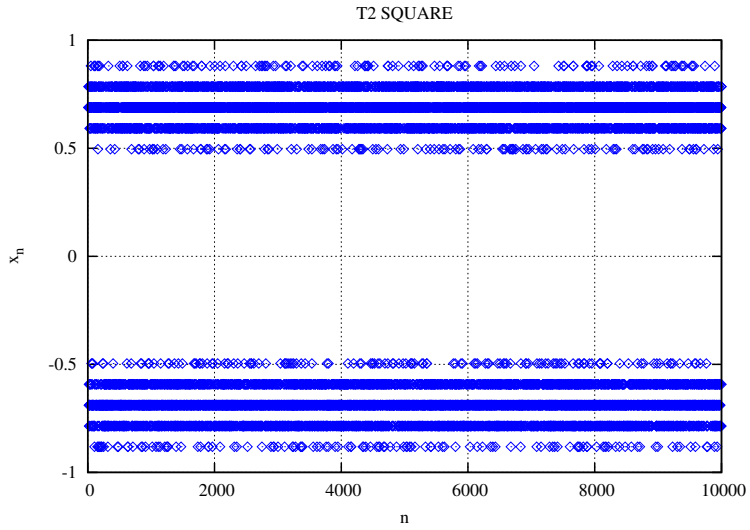

Figure 8: Samples x_n at the input of the zero threshold detector of the telemetry receiver. Case of codes T2 or T2B, $h(t) = h_{sq}(t)$; $m_{TM} = 1.25$ and $m_{RG} = 0.7$, ideal transponder.

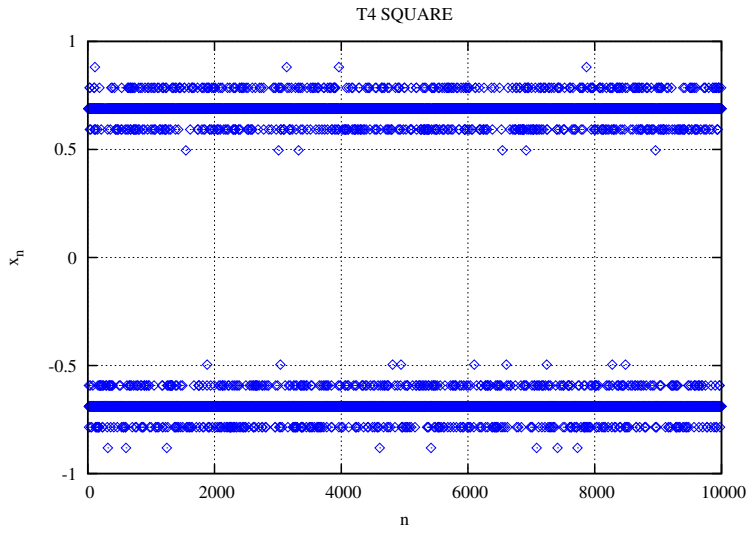

Figure 9: Samples x_n at the input of the zero threshold detector of the telemetry receiver. Case of codes T4 or T4B, $h(t) = h_{sq}(t)$; $m_{TM} = 1.25$ and $m_{RG} = 0.7$, ideal transponder.

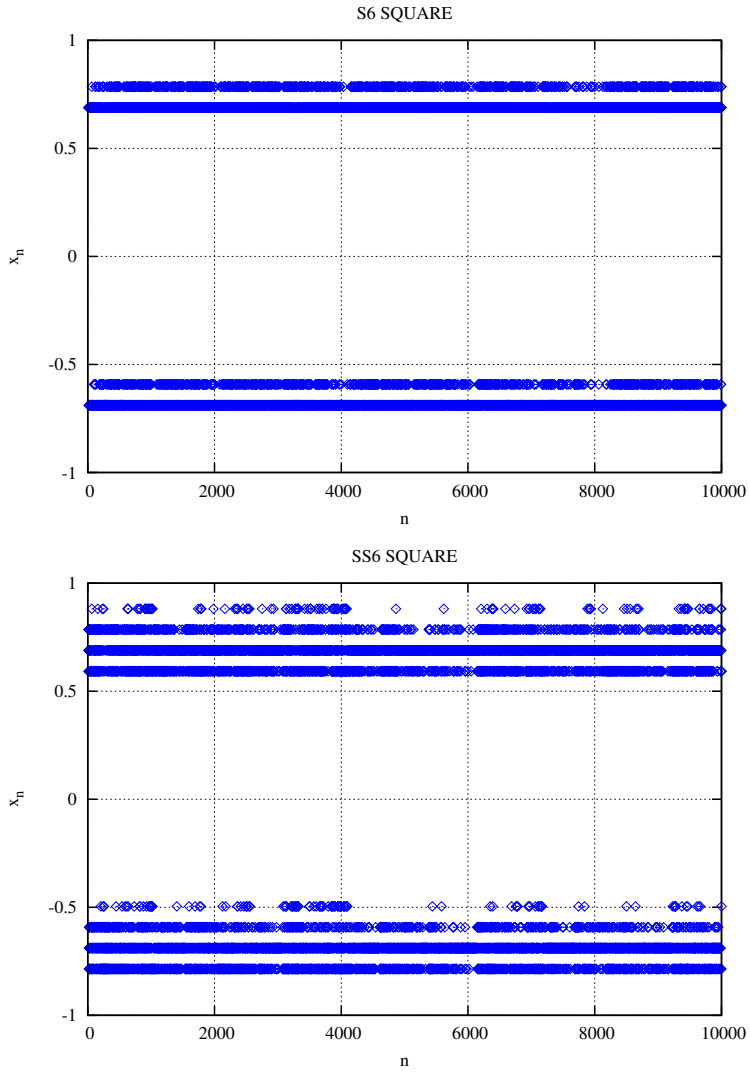

Figure 10: Samples x_n at the input of the zero threshold detector of the telemetry receiver. Case of codes S6 and SS6 (or S8 and SS8), $h(t) = h_{sq}(t)$; $m_{TM} = 1.25$ and $m_{RG} = 0.7$, ideal transponder.

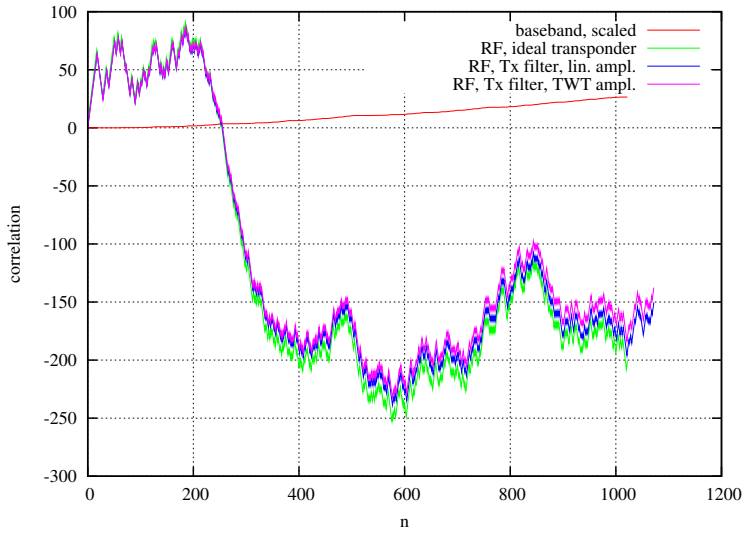

Figure 11: Correlation between the received signal and probing signal $p_2(t)$ as a function of time; case of code S6, $h(t) = h_{sq}(t)$, $m_{TM} = 1.25$ and $m_{RG} = 0.2$, no noise, for a baseband system (no interference from the telemetry system), and for the RF system with ideal and realistic transponder.

2.6.2 The ranging system

Regarding the ranging system, again some special considerations are necessary for the Stiffler codes. The unscrambled Stiffler ranging signal is generated as

$$s_r(t) = \text{sign}\left(vp_1(t) + \sum_{i=2}^{20} p_i(t)\right), \tag{42}$$

where v is the clock vote (either 6 or 8 in this analysis), and $p_i(t)$ is a periodic square wave with period $2^i T_{RG}$ chips. The ranging code phase detector evaluates the correlation between the received signal and each of the probing signals $p_i(t)$ for $i = 1, \ldots, 20$ and takes binary decisions to establish whether $p_i(t)$ or $-p_i(t)$ is the received component. It has to be noticed that, having set the chip rate equal to $R_{RG} = 2$ Mchip/s and the telemetry bit rate equal to $R_{TM} = 500$ kbit/s, $p_2(t)$ exactly corresponds to the SP-L pulse $p_{TM}(t)$ of the telemetry signal. Thus the telemetry signal highly influences the correlation between $p_2(t)$ and the received signal. Figure 11 shows the evolution of the correlation between the received signal and probing signal $p_2(t)$ as a function of the integration time. It can be easily noticed that the correlation dramatically changes in the presence of the telemetry signal, even for the ideal transponder; only marginal changes are introduced by the TX filter and by the TX filter plus the TWTA. Actually, the shown correlation is simply the sum of the samples x_n shown in figure 10 (upper plot) where the sample polarity is determined by the telemetry bit, while the ranging chips give rise to the small variations. If the number of zeros and ones is equal in the telemetry bit sequence in the considered integration interval, then the telemetry effects are cancelled out; but large consecutive runs of zeros or ones generate strong variations in the correlation values at local level, as shown in figure 11. All the simulations related to the performance of the Stiffler ranging system were evaluated using a telemetry bit sequence with period $2^{18} - 1$ and $2^{17} + 1$ ones and $2^{17} - 1$ zeros in the ranging signal observation time (2^{20} chips, i.e. 2^{18} telemetry bits). Thus the effects of the telemetry bits are almost eliminated in the simulations, at least for the case

of ideal transponder. Some effects are however present with the realistic transponder, since the evolution of the correlation is slightly different, as shown in figure 11.

The scrambled Stiffler codes suffer from the same problem since the scrambling simply delays by two chips signal $p_2(t)$ (thus changes $p_2(t)$ into $-p_2(t)$).

Notice that this problem occurs for the unscrambled Stiffler codes any time $R_{TM} = R_{RG}/2^k$, since the telemetry bits affect the correlation between the received signal and the probing signal $p_k(t)$. The interference between telemetry and ranging for other values of R_{TM} and R_{RG} has to be still analyzed.

3 Results for the ideal transponder

In the following sections, the semianalytical error probabilities for ranging, telecommand and telemetry are given assuming that the transponder is ideal (no input and output filters, linear amplifier). The results are first given for the uplink (telecommand and ranging, with $m_{TC} = 1$ and $m_{RG} = 0.7$) and then for the downlink (telemetry and ranging, with $m_{TM} = 1.25$ and $m_{RG} = 0.7, 0.5$ and 0.2).

3.1 Uplink with $m_{TC} = 1$ and $m_{RG} = 0.7$

The telecommand error probability is almost unaffected by the presence of the interfering ranging signal, and very small differences can be noticed among the various ranging codes, as can be seen from figures 12 and 13. From table 3 it is possible to notice that the losses with respect to the ideal 2-PAM system are less than 0.2 dB; the higher losses are obtained for code S6. When $h(t) = h_{sin}(t)$ slightly larger losses are present, all of them larger than 0.0385 dB, which is the minimum loss due to the unmatched filter in the telecommand receiver, as from eqn. (19).

The detected phase of the ranging code is wrong with a probability given in figures 14 and 15 for the Stiffler and Tausworthe codes, respectively. The losses measured at $P_{RG}(e) = 10^{-6}$ are listed in table 4; the theoretical losses due to the non-ideal receiver are approximately equal to 0.191 dB for $h(t) = h_{sq}(t)$ and 1.045 dB for $h(t) = h_{sin}(t)$ (see sect. 2.5), and these value are practically respected, which means that the telecommand interference introduces negligible losses, apart from the case of codes JPL99 and S6 with $h(t) = h_{sq}(t)$.

code	$h(t) = h_{sq}(t)$	$h(t) = h_{sin}(t)$
JPL99	0.022	0.056
T2	0.034	0.057
T2B	0.042	0.062
T4	0.025	0.056
T4B	0.020	0.054
S6	0.186	0.108
SS6	0.034	0.059
S8	0.084	0.073
SS8	0.020	0.055

Table 3: Uplink losses at $P_{TC}(e) = 10^{-4}$ for the telecommand system, with the various codes; $m_{RG} = 0.7$ and $m_{TC} = 1.0$, ideal transponder.

code	$h(t) = h_{sq}(t)$	$h(t) = h_{sin}(t)$
JPL99	0.223	1.111
T2	0.194	1.077
T2B	0.189	1.070
T4	0.186	1.081
T4B	0.191	1.065
S6	0.454	1.056
SS6	0.162	1.046
S8	0.162	1.098
SS8	0.152	1.045

Table 4: Uplink losses for the ranging system, with the various codes; $m_{RG} = 0.7$ and $m_{TC} = 1$, ideal transponder.

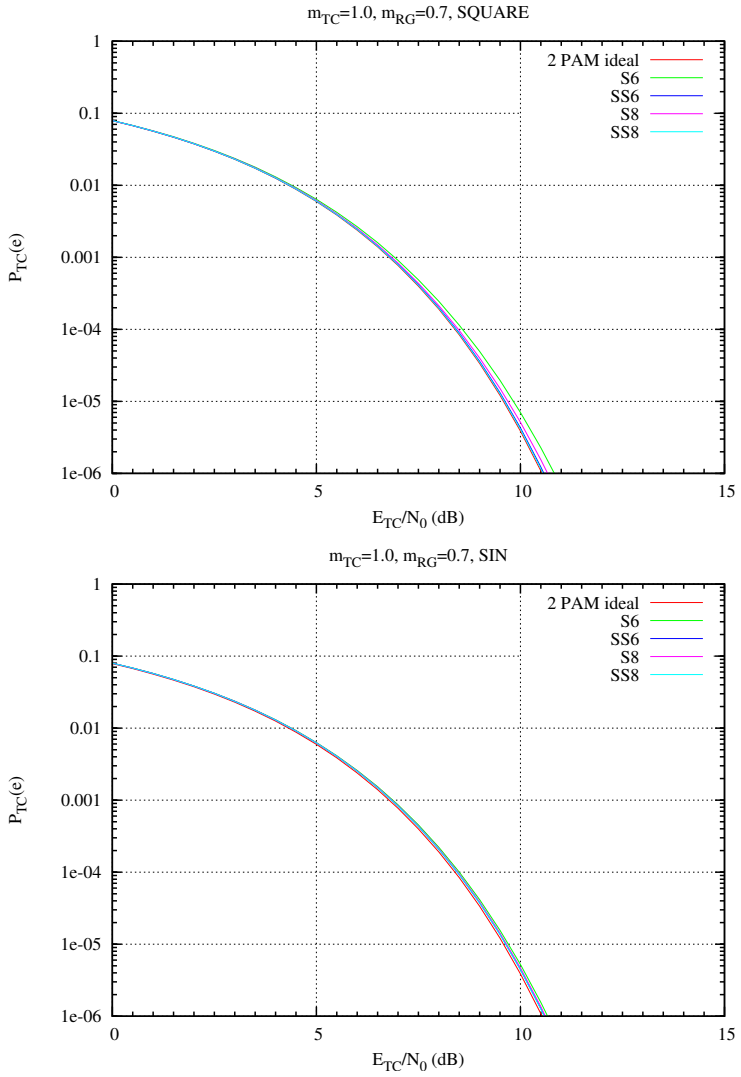

Figure 12: Error probability for telecommand with the interference of the ranging signal. Case of Stiffler codes, $h(t) = h_{sq}(t)$ (upper graph) and $h(t) = h_{sin}(t)$ (lower graph); $m_{TC} = 1$ and $m_{RG} = 0.7$, ideal transponder.

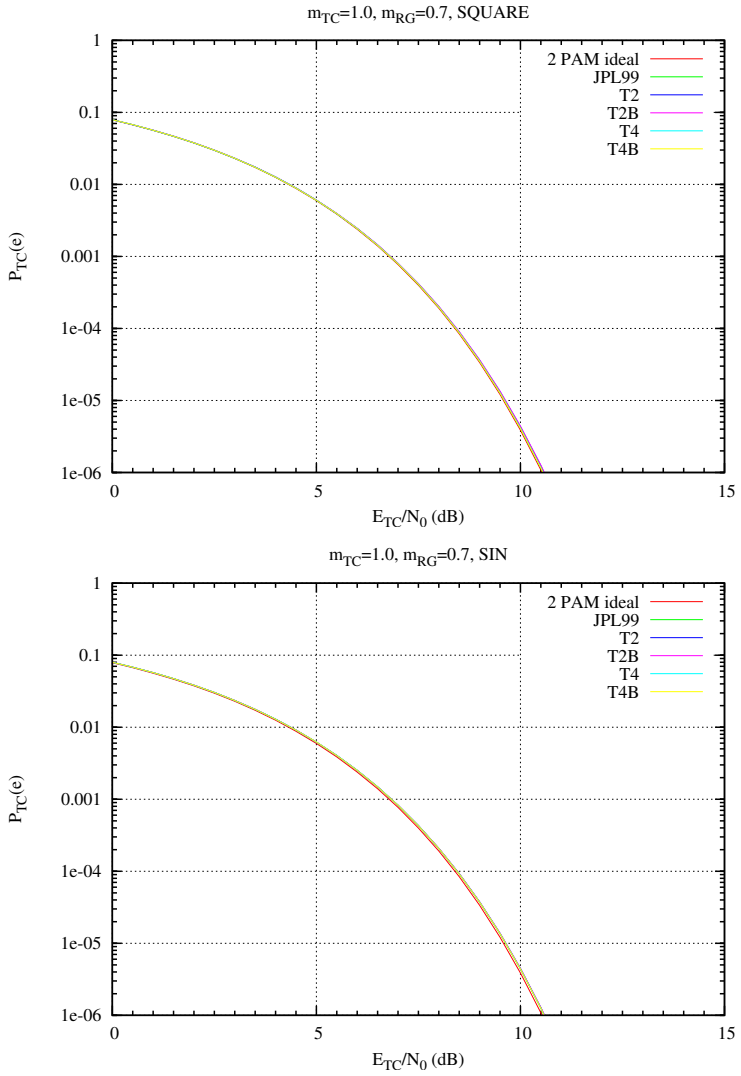

Figure 13: Error probability for telecommand with the interference of the ranging signal. Case of Tausworthe codes, $h(t) = h_{sq}(t)$ (upper graph) and $h(t) = h_{sin}(t)$ (lower graph); $m_{TC} = 1$ and $m_{RG} = 0.7$, ideal transponder.

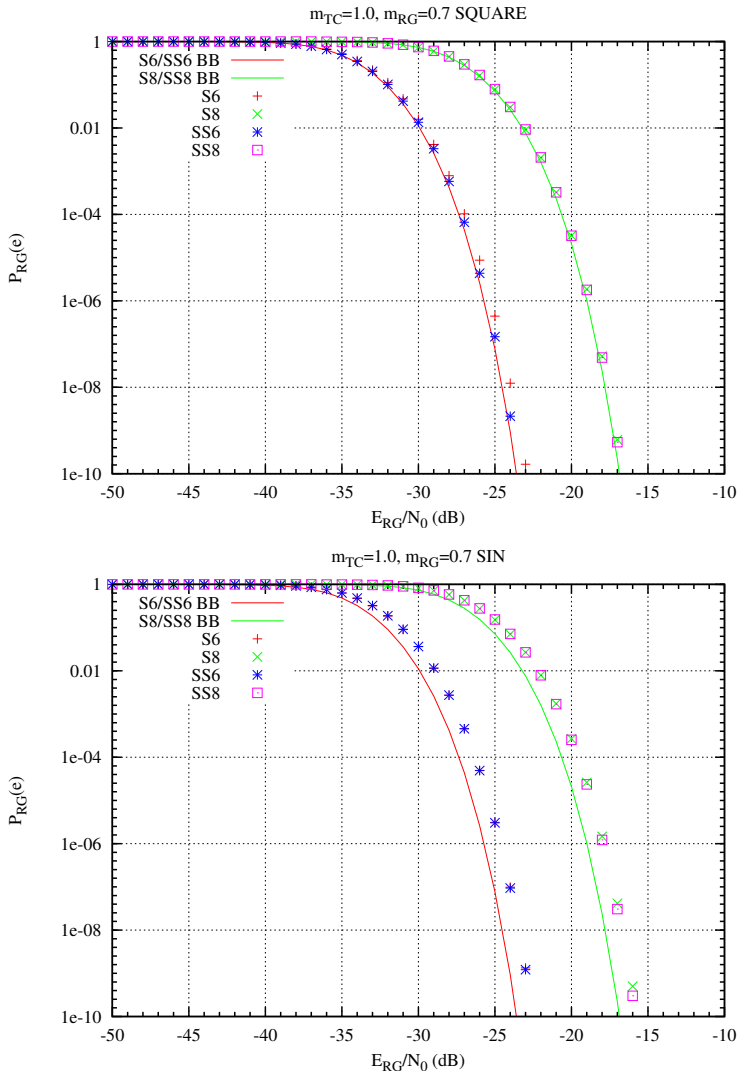

Figure 14: Error probability for the ranging system with the interference of the telecommand signal. Case of Stiffler codes observed for one ranging period, $h(t) = h_{sq}(t)$ (upper graph) and $h(t) = h_{sin}(t)$ (lower graph), $m_{TC} = 1$ and $m_{RG} = 0.7$, ideal transponder.

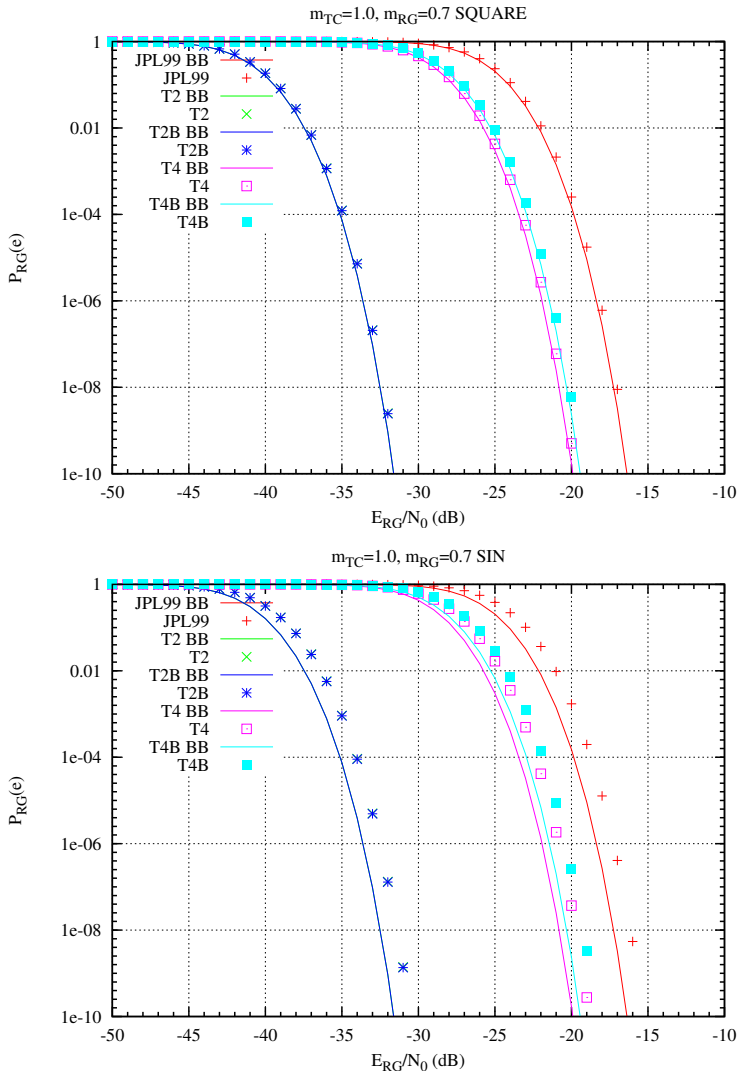

Figure 15: Error probability for the ranging system with the interference of the telecommand signal. Case of Tausworthe codes observed for one ranging period, serial receiver, $h(t) = h_{sq}(t)$ (upper graph) and $h(t) = h_{sin}(t)$ (lower graph), $m_{TC} = 1$ and $m_{RG} = 0.7$, ideal transponder.

3.2 Downlink with $m_{TM} = 1.25$ and $m_{RG} = 0.7$

Figures 16 and 17 show the telemetry error probability in the presence of the Stiffler and Tautsworth ranging codes, respectively. Tables 5 and 6 allow for a better comparison between the semianalytical (SA) error probabilities and the Monte Carlo (MC) bit error rates obtained by ESTEC (see [1]). The two techniques used to measure the telemetry error rates give very similar results, thus cross-validating each other. Some differences are present for code T2B and SS6 at $E_{TM}/N_0 = 10$ and 11 dB; as for code SS6, we already explained that the error probabilities strongly depend on the telemetry bit sequence for such high values of the signal to noise ratios, while further analysis is in progress for code T2B. Table 8 lists the losses for the telemetry system with respect to the ideal 2-PAM performance: codes T2, T2B and SS6 show the worst performance, especially for $h(t) = h_{sq}(t)$, while the other codes are practically equivalent.

However, when the ranging system performance is considered (see figs. 18 and 19 and table 9), we see that codes T2 and T2B are the most robust against the telemetry interference together with codes S6 and S8, followed by codes SS6, T4B, T4, SS8 and JPL99.

code	$E_{TM}/N_0 = 6$ dB	7 dB	8 dB	9 dB	10 dB	11 dB
JPL99 - SA	2.539e-3	8.527e-4	2.243e-4	4.407e-5	6.160e-6	5.865e-7
JPL99 - MC	2.6e-3	9.1e-4	2.5e-4	4.9e-5	-	-
T2 - SA	3.560e-3	1.420e-3	4.820e-4	1.364e-4	3.151e-5	5.770e-6
T2 - MC	3.3e-3	1.2e-3	3.8e-4	1.1e-4	-	-
T2B - SA	3.562e-3	1.424e-3	4.854e-4	1.385e-4	3.244e-5	6.043e-6
T2B - MC	3.4e-3	1.3e-3	4.5e-4	1.0e-4	2e-5	4.1e-6
T4 - SA	2.612e-3	8.930e-4	2.422e-4	5.023e-5	7.763e-6	8.925e-7
T4 - MC	2.7e-3	9.2e-4	2.6e-4	5.2e-5	-	-
T4B - SA	2.599e-3	8.859e-4	2.392e-4	4.932e-5	7.574e-6	8.688e-7
T4B - MC	2.6e-3	9.1e-4	2.6e-4	4.7e-5	-	-
S6 - SA	2.634e-3	9.030e-4	2.452e-4	5.057e-5	7.578e-6	7.877e-7
S6 - MC	2.6e-3	9.2e-4	2.6e-4	5.1e-5	-	-
SS6 - SA	2.926e-3	1.063e-3	3.174e-4	7.600e-5	1.440e-5	2.143e-6
SS6 - MC	2.9e-3	1.0e-3	3.3e-4	7.1e-5	9e-6	1.5e-6
S8 - SA	2.498e-3	8.314e-4	2.154e-4	4.131e-5	5.555e-6	5.007e-7
S8 - MC	2.5e-3	8.7e-4	2.2e-4	4.1e-5	-	-
SS8 - SA	2.603e-3	8.874e-4	2.394e-4	4.912e-5	7.418e-6	8.123e-7
SS8 - MC	2.6e-3	9.0e-4	2.5e-4	4.9e-5	-	-

Table 5: Tausworthe and Stiffler ranging codes with $h(t) = h_{sq}(t)$, $m_{RG} = 0.7$, and telemetry data with $m_{TM} = 1.25$, ideal transponder. Comparison between the semianalytical (SA) error probabilities for telemetry and the bit error rates (MC) measured by ESTEC with the Monte Carlo technique.

code	$E_{TM}/N_0 = 6$ dB	7 dB	8 dB	9 dB	10 dB	11 dB
JPL99 - SA	2.52e-3	8.350e-4	2.124e-4	3.908e-5	4.811e-06	3.614e-7
JPL99 - MC	2.5e-3	8.5e-4	2.1e-4	3.9e-5	-	-
T2 - SA	2.837e-3	9.966e-4	2.789e-4	5.942e-5	9.135e-6	9.539e-7
T2 - MC	2.7e-3	9.5e-4	2.6e-4	5.8e-5	-	-
T2B - SA	2.836e-3	9.965e-4	2.791e-4	5.955e-5	9.189e-6	9.668e-7
T2B - MC	2.8e-3	1.1e-3	2.8e-4	5.3e-5	-	-
T4 - SA	2.552e-3	8.467e-4	2.172e-4	4.052e-5	5.111e-6	4.011e-7
T4 - MC	2.5e-3	8.5e-4	2.1e-4	4.0e-5	-	-
T4B - SA	2.548e-3	8.446e-4	2.163e-4	4.027e-5	5.061e-6	3.952e-7
T4B - MC	2.5e-3	8.7e-4	2.2e-4	3.9e-5	-	-
S6 - SA	2.560e-3	8.507e-4	2.186e-4	4.088e-5	5.165e-6	4.039e-7
S6 - MC	2.5e-3	8.7e-4	2.3e-4	4.1e-5	-	-
SS6 - SA	2.648e-3	8.969e-4	2.376e-4	4.664e-5	6.376e-6	5.673e-7
SS6 - MC	2.6e-3	9.1e-4	2.7e-4	4.4e-5	-	-
S8 - SA	2.516e-3	8.284e-4	2.098e-4	3.831e-5	4.661e-6	3.433e-7
S8 - MC	2.5e-3	8.6e-4	2.2e-4	3.9e-5	-	-
SS8 - SA	2.549e-3	8.453e-4	2.166e-4	4.032e-5	5.065e-6	3.941e-7
SS8 - MC	2.5e-3	8.6e-4	2.2e-4	3.9e-5	-	-

Table 6: Tausworthe and Stiffler ranging codes with $h(t) = h_{sin}(t)$, $m_{RG} = 0.7$, and telemetry data with $m_{TM} = 1.25$, ideal transponder. Comparison between the semianalytical (SA) error probabilities for telemetry and the bit error rates (MC) measured by ESTEC with the Monte Carlo technique.

code	$E_{TM}/N_0 = 6$ dB	7 dB	8 dB	9 dB	10 dB	11 dB
JPL99 - SA	2.434e-3	7.963e-4	2.003e-4	3.634e-5	4.398e-6	3.234e-7
JPL99 - MC	2.5e-3	8.5e-4	2.1e-4	3.9e-5	-	-
T2 - SA	2.735e-3	9.532e-4	2.642e-4	5.564e-5	8.437e-6	8.669e-7
T2 - MC	2.7e-3	9.5e-4	2.6e-4	5.8e-5	-	-
T2B - SA	2.734e-3	9.532e-4	2.644e-4	5.577e-5	8.489e-6	8.790e-7
T2B - MC	2.8e-3	1.1e-3	2.8e-4	5.3e-5	-	-
T4 - SA	2.552e-3	8.467e-4	2.172e-4	4.052e-5	5.111e-6	4.011e-7
T4 - MC	2.5e-3	8.5e-4	2.1e-4	4.0e-5	-	-
T4B - SA	2.452e-3	8.056e-4	2.040e-4	3.747e-5	4.631e-6	3.544e-7
T4B - MC	2.5e-3	8.7e-4	2.2e-4	3.9e-5	-	-
S6 - SA	2.464e-3	8.115e-4	2.062e-4	3.805e-5	4.727e-6	3.621e-7
S6 - MC	2.5e-3	8.7e-4	2.3e-4	4.1e-5	-	-
SS6 - SA	2.550e-3	8.563e-4	2.245e-4	4.351e-5	5.858e-6	5.120e-7
SS6 - MC	2.6e-3	9.1e-4	2.7e-4	4.4e-5	-	-
S8 - SA	2.421e-3	7.899e-4	1.977e-4	3.561e-5	4.258e-6	3.070e-7
S8 - MC	2.5e-3	8.6e-4	2.2e-4	3.9e-5	-	-
SS8 - SA	2.453e-3	8.063e-4	2.043e-4	3.752e-5	4.634e-6	3.533e-7
SS8 - MC	2.5e-3	8.6e-4	2.2e-4	3.9e-5	-	-

Table 7: Tausworthe and Stiffler ranging codes with $h(t) = h_{sin}(t)$, $m_{RG} = 0.7$, and telemetry data with $m_{TM} = 1.25$, ideal transponder. Comparison between the semianalytical (SA) error probabilities for telemetry and the bit error rates (MC) measured by ESTEC with the Monte Carlo technique. ESA definition of P_{TM}.

code	$h(t) = h_{sq}(t)$	$h(t) = h_{sin}(t)$
JPL99	0.126	0.076
T2	0.826	0.285
T2B	0.839	0.286
T4	0.187	0.093
T4B	0.178	0.090
S6	0.193	0.098
SS6	0.421	0.160
S8	0.095	0.066
SS8	0.177	0.091

Table 8: Downlink losses at $P_{TM}(e) = 10^{-4}$ for the telemetry system, with the various codes; $m_{RG} = 0.7$ and $m_{TM} = 1.25$, ideal transponder.

code	$h(t) = h_{sq}(t)$	$h(t) = h_{sin}(t)$
JPL99	1.136	2.070
T2	0.065	0.108
T2B	0.060	0.100
T4	0.606	1.048
T4B	0.631	1.157
S6	0.000	0.000
SS6	0.127	0.282
S8	0.000	0.004
SS8	0.760	1.452

Table 9: Downlink losses at $P_{RG}(e) = 10^{-6}$ for the ranging system, with the various codes; $m_{RG} = 0.7$ and $m_{TM} = 1.25$, ideal transponder.

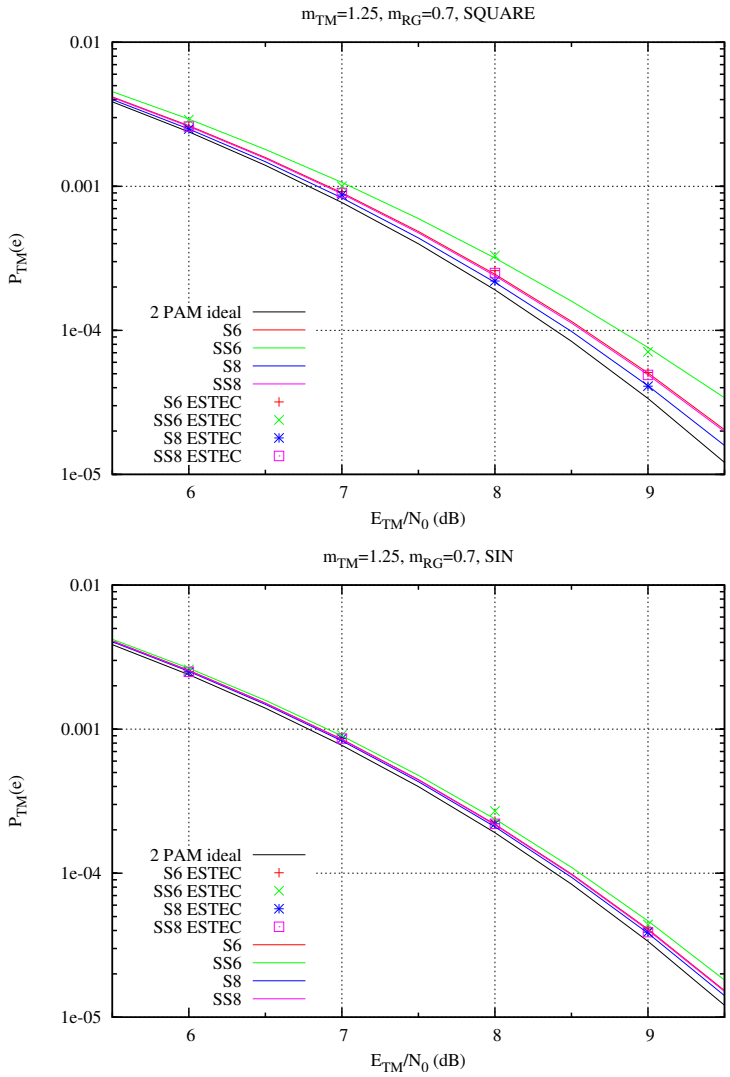

Figure 16: Error probability for telemetry with the interference of the ranging signal. Case of Stiffler codes, $h(t) = h_{sq}(t)$ (upper graph) and $h(t) = h_{sin}(t)$ (lower graph); $m_{TM} = 1.25$ and $m_{RG} = 0.7$, ideal transponder.

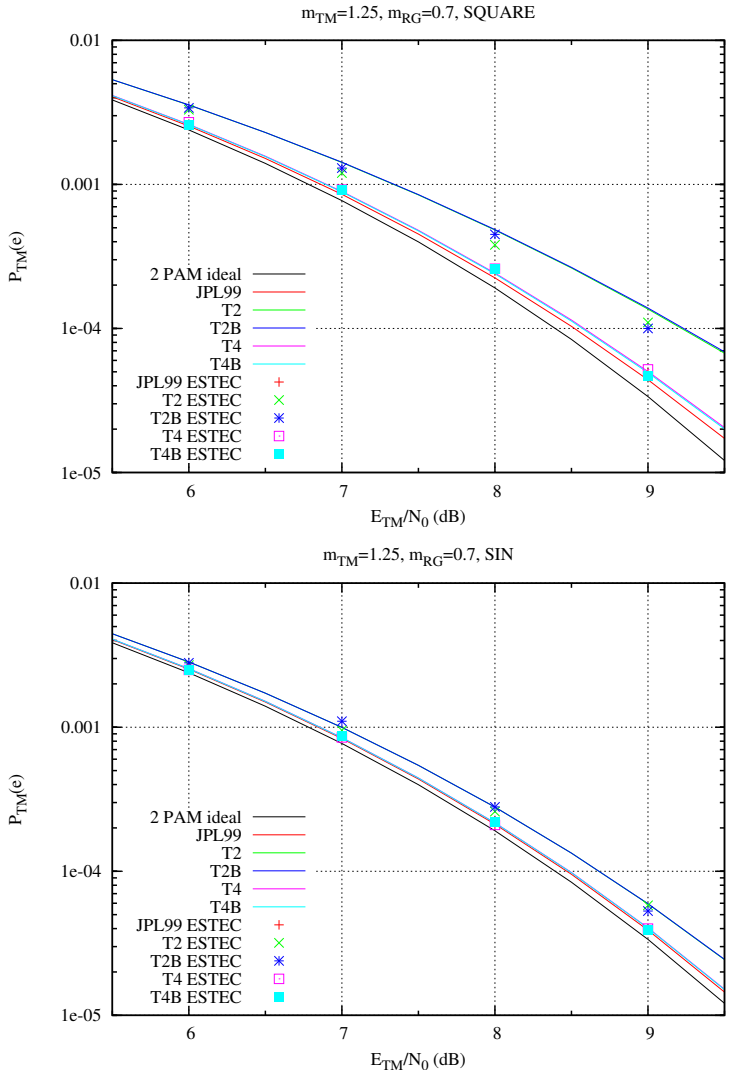

Figure 17: Error probability for telemetry with the interference of the ranging signal. Case of Tautsworth codes, $h(t) = h_{sq}(t)$ (upper graph) and $h(t) = h_{sin}(t)$ (lower graph); $m_{TM} = 1.25$ and $m_{RG} = 0.7$, ideal transponder.

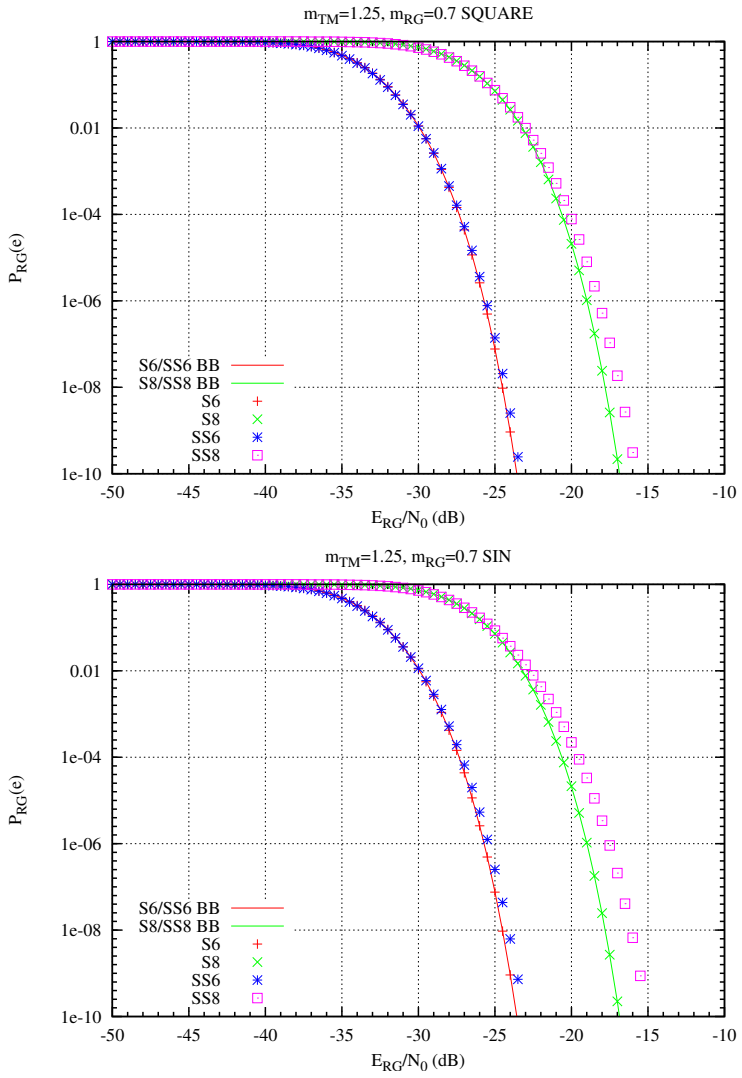

Figure 18: Error probability for the ranging system with the interference of the telemetry signal. Case of Stiffler codes observed for one ranging period, parallel receiver, $h(t) = h_{sq}(t)$ (upper graph) and $h(t) = h_{sin}(t)$ (lower graph), $m_{TM} = 1.25$ and $m_{RG} = 0.7$, ideal transponder.

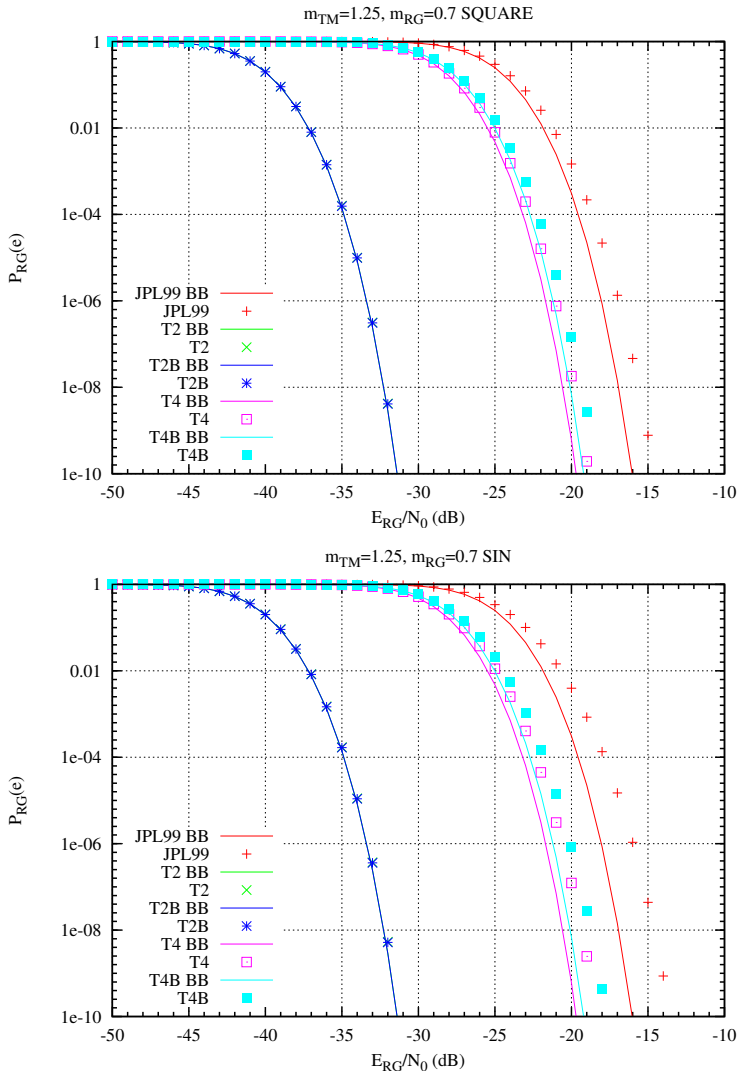

Figure 19: Error probability for the ranging system with the interference of the telemetry signal. Case of Tausworthe codes observed for one ranging period, parallel receiver, $h(t) = h_{sq}(t)$ (upper graph) and $h(t) = h_{sin}(t)$ (lower graph), $m_{TM} = 1.25$ and $m_{RG} = 0.7$, ideal transponder.

3.3 Downlink with $m_{TM} = 1.25$ and $m_{RG} = 0.5$

A reduced value of m_{RG} allows for smaller losses for the telemetry system (see figs. 20 and 21, and table 10). Codes T2 and T2B continue to produce a non-negligible loss on the telemetry system, while the other Tausworthe codes practically behave as the Stiffler codes. The ranging system, on the contrary, is more affected by the interfering telemetry signal, as shown in figures 22 and 23 (see also table 11): as for the case $m_{RG} = 0.7$, the losses for codes S6, S8, T2 and T2B are almost negligible, while the other Tausworthe codes show high losses, especially in the case $h(t) = h_{sin}(t)$.

code	$h(t) = h_{sq}(t)$	$h(t) = h_{sin}(t)$
JPL99	0.048	0.026
T2	0.326	0.128
T2B	0.328	0.128
T4	0.071	0.033
T4B	0.067	0.032
S6	0.077	0.036
SS6	0.162	0.067
S8	0.035	0.021
SS8	0.068	0.032

Table 10: Downlink losses at $P_{TM}(e) = 10^{-4}$ for the telemetry system, with the various codes; $m_{RG} = 0.5$ and $m_{TM} = 1.25$, ideal transponder.

code	$h(t) = h_{sq}(t)$	$h(t) = h_{sin}(t)$
JPL99	2.519	4.211
T2	0.131	0.208
T2B	0.121	0.194
T4	1.279	2.092
T4B	1.406	2.325
S6	0.000	0.000
SS6	0.343	0.676
S8	0.000	0.003
SS8	1.743	2.847

Table 11: Downlink losses at $P_{RG}(e) = 10^{-6}$ for the ranging system, with the variouscodes; $m_{RG} = 0.5$ and $m_{TM} = 1.25$, ideal transponder.

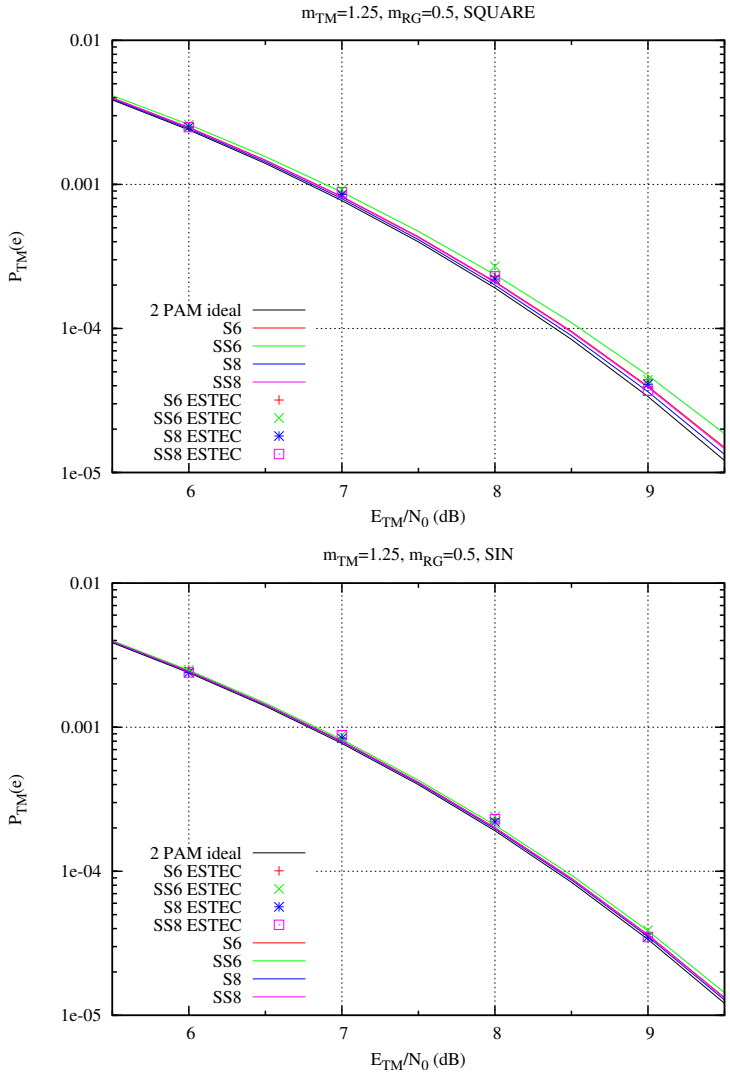

Figure 20: Error probability for telemetry with the interference of the ranging signal. Case of Stiffler codes, $h(t) = h_{sq}(t)$ (upper graph) and $h(t) = h_{sin}(t)$ (lower graph); $m_{TM} = 1.25$ and $m_{RG} = 0.5$, ideal transponder.

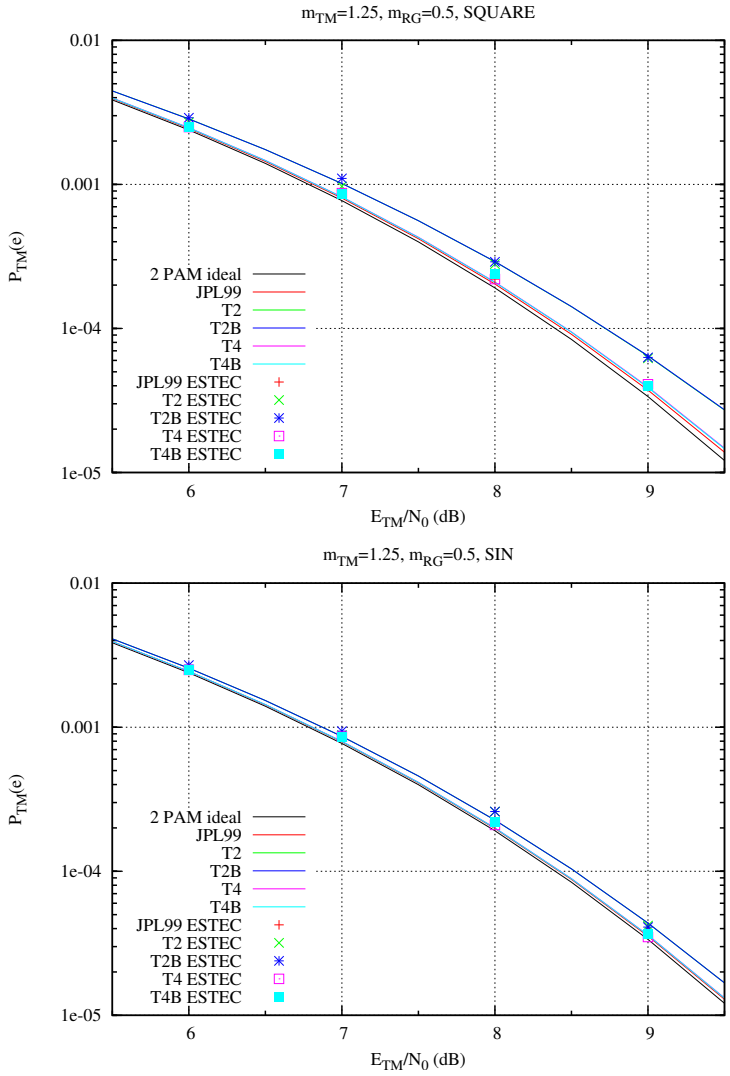

Figure 21: Error probability for telemetry with the interference of the ranging signal. Case of Tausworthe codes, $h(t) = h_{sq}(t)$ (upper graph) and $h(t) = h_{sin}(t)$ (lower graph); $m_{TM} = 1.25$ and $m_{RG} = 0.5$, ideal transponder.

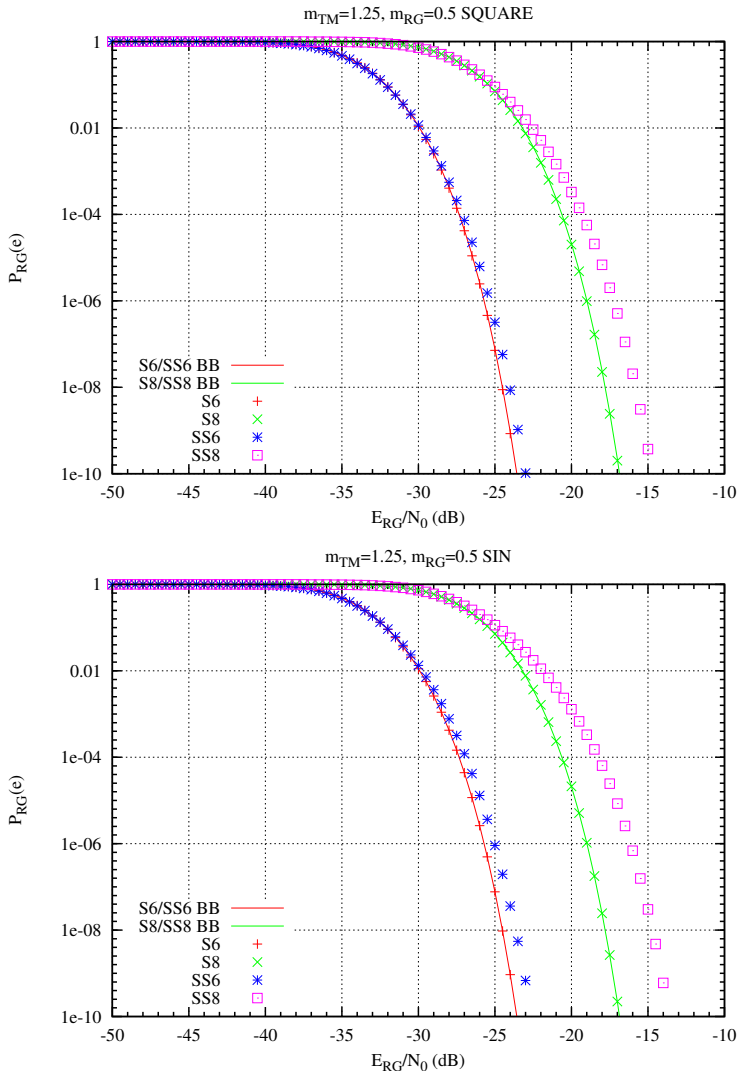

Figure 22: Error probability for the ranging system with the interference of the telemetry signal. Case of Stiffler codes observed for one ranging period, parallel receiver, $h(t) = h_{sq}(t)$ (upper graph) and $h(t) = h_{sin}(t)$ (lower graph), $m_{TM} = 1.25$ and $m_{RG} = 0.5$, ideal transponder.

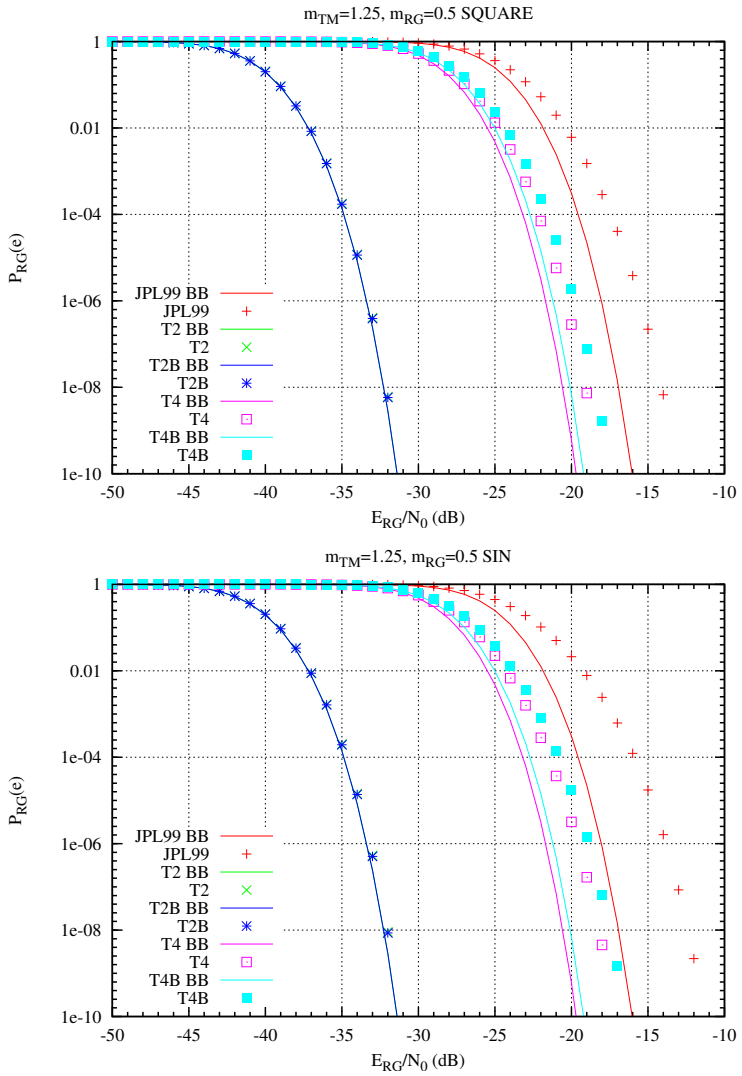

Figure 23: Error probability for the ranging system with the interference of the telemetry signal. Case of Tausworthe codes observed for one ranging period, parallel receiver, $h(t) = h_{sq}(t)$ (upper graph) and $h(t) = h_{sin}(t)$ (lower graph), $m_{TM} = 1.25$ and $m_{RG} = 0.5$, ideal transponder.

IBO (dB)	OBO (dB)	Phase rotation (deg)
-20	-12.59	-0.
-19	-11.47	-0.02
-18	-10.48	-0.49
-17	-9.54	-0.97
-16	-8.63	-1.63
-15	-7.78	-2.39
-14	-6.90	-3.55
-13	-6.02	-5.02
-12	-5.15	-6.91
-11	-4.34	-9.11
-10	-3.58	-11.74
- 9	-2.91	-14.65
- 8	-2.30	-17.67
- 7	-1.75	-21.09
- 6	-1.30	-24.78
- 5	-0.94	-28.40
- 4	-0.69	-32.22
- 3	-0.50	-35.97
- 2	-0.35	-39.89
- 1	-0.21	-43.67
0	-0.00	-47.56

Table 12: Output backoff (OBO) and phase rotation as functions of the input backoff (IBO) for the 35 W TWTA under analysis.

3.4 Conclusions

Figures 24 and 25 show the losses for the telemetry and ranging systems for $m_{RG} = 0.2, 0.5, 0.7$, for the case of $h(t) = h_{sq}(t)$ and $h(t) = h_{sin}(t)$.

In general, waveform $h_{sq}(t)$ generates smaller losses for the ranging system and higher losses for the telemetry system, so that the choice between the two is difficult.

When considering the losses, it is apparent that codes S6 and S8 are the best compromise in terms of both the telemetry and ranging systems. Among the Tausworthe codes, the best compromise seem to be codes T4 and T4B. In fact codes T2/T2B practically do not suffer from the presence of the telemetry interference, but generate large losses on the telemetry system. Code JPL99 gives rise to the largest losses for the ranging system, while it is slightly better than codes T4/T4B as far as the telemetry is concerned. When E_{RG}/N_0 is also considered (smaller values correspond to faster ranging phase acquisition), then we see that code S6 should be preferred to codes S8, T4 and T4B.

4 Realistic transponder

The satellite transponder is not ideal, and, in particular the input (RX) filter, the output (TX) filter and the amplifier should be adequately described. The satellite transmitter is made of: the ideal phase modulator followed by the TX filter and then by the nonlinear amplifier. As for the nonlinear amplifier, a 35 W TWTA (Travelling Wave Tube Amplifier) is considered, using the AM/AM and AM/PM characteristics given in table 12, which are also shown in figure 26.

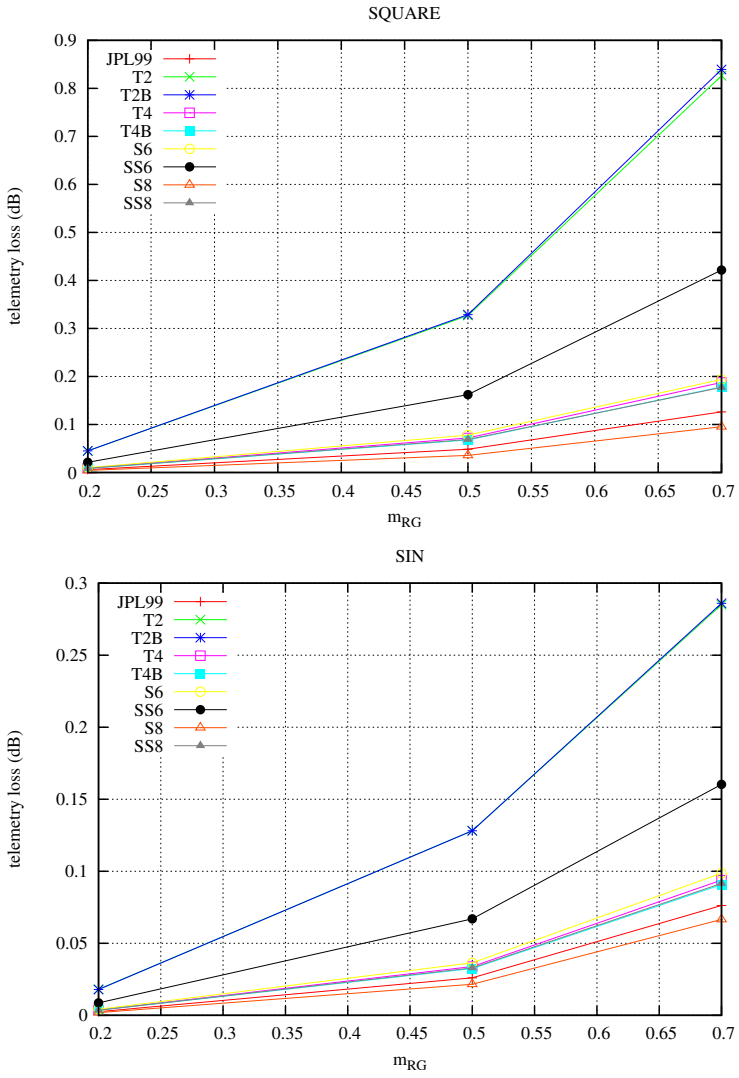

Figure 24: Losses for the telemetry system at $P_{TM}(e) = 10^{-4}$ as function of m_{RG} for the various codes, $h(t) = h_{sq}(t)$ (upper graph) and $h(t) = h_{sin}(t)$ (lower graph), $m_{TM} = 1.25$ ideal transponder.

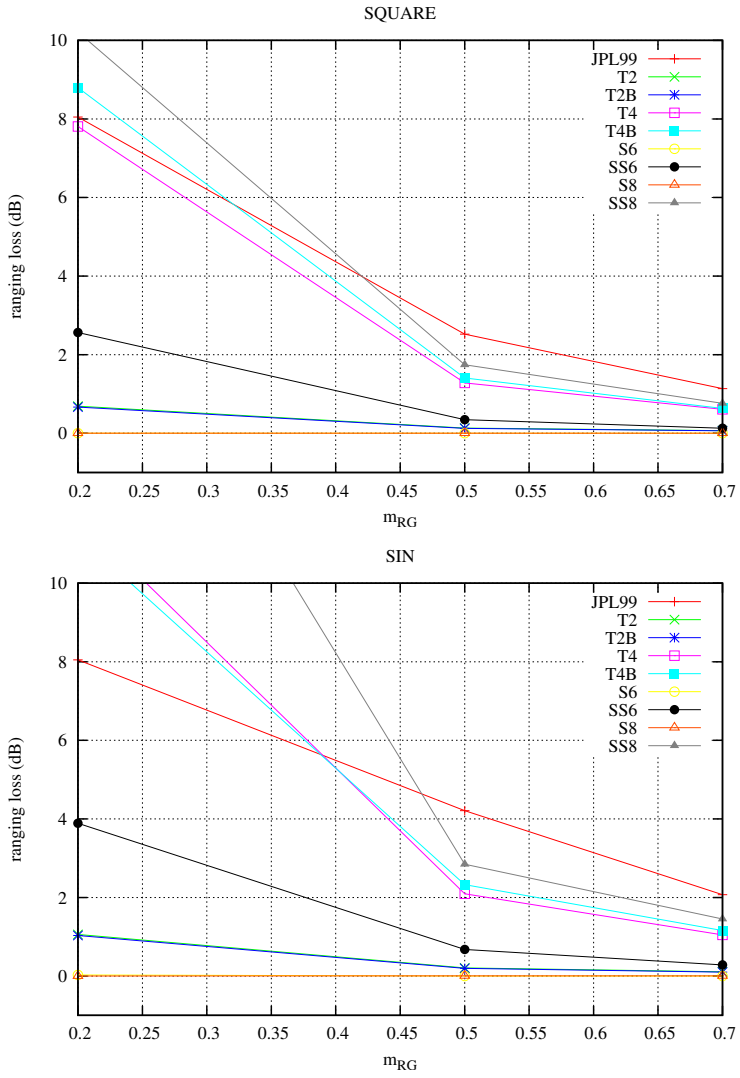

Figure 25: Losses for the ranging system at $P_{RG}(e) = 10^{-6}$ as function of m_{RG} for the various codes, $h(t) = h_{sq}(t)$ (upper graph) and $h(t) = h_{sin}(t)$ (lower graph), $m_{TM} = 1.25$ ideal transponder.

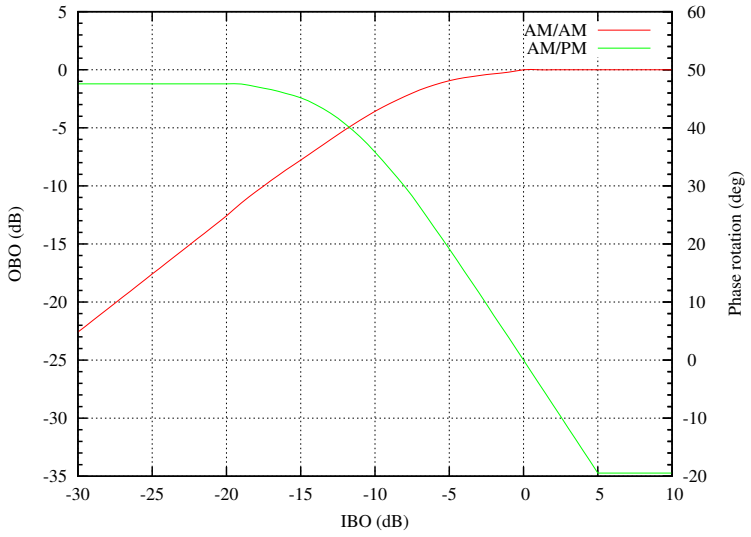

Figure 26: AM/AM and AM/PM characteristics of the 35 W TWTA as measured by simulation.

Parameter	Value	Unit	
1 dB bandwidth	7	MHz	Min
3 dB bandwidth	7.5	MHz	Max
50 dB bandwidth	12	MHz	Max
Amplitude in-band ripple	0.2	dB	Max
Amplitude in-band slope	±0.1	dB/MHz	Max
Phase in-band ripple	6	deg P-P	Max
Group delay in-band ripple	30	ns P-P	Max
Triple transit suppression	60	dB	Min

Table 13: On-board TX filter specifications.

As for the TX/RX filters, the specifications are given in tables 13 and 14.

These filters have been simulated through two cascaded filters. The first filter is a linear phase raised cosine filter with theoretical baseband frequency response

$$H(f) = \begin{cases} T & |f| < (1-\rho)/(2T) \\ \frac{T}{2}\left\{1 - \sin\left[\frac{\pi T}{\rho}\left(|f| - \frac{1}{2T}\right)\right]\right\} & (1-\rho)/(2T) < |f| < (1+\rho)/(2T) \\ 0 & |f| > (1+\rho)/(2T) \end{cases}$$

For the TX filter we used $\rho = 0.2$ and $1/(2T) = 4$ MHz; for the RX filter we used $\rho = 0.1$ and $1/(2T) = 3.2$ MHz; each filter was simulated through an FIR filter with 60 taps, having set 16 samples per chip interval.

The SAW filters, which are considered for the on-board transponder, are characterized by a periodic group delay ripple. The input signal takes a time T_T to transit through the physical device, but part of the signal is reflected and exits the device after a further time equal to $2T_T$; thus at the output we have a desired signal, delayed by T_T, plus a spurious signal delayed by $3T_T$ (triple-transit time). The modelling of this phenomenon can be easily taken into account by introducing a new filter with impulse response

$$h_g(t) = A_1\delta(t - T_T) + A_2\delta(t - 3T_T)$$

Parameter	Value	Unit	
1 dB bandwidth	6	MHz	Min
3 dB bandwidth	6.6	MHz	Min
50 dB bandwidth	8	MHz	Max
Amplitude in-band ripple	0.4	dB	Max
Amplitude in-band slope	±0.1	dB/MHz	Max
Phase in-band ripple	6	deg P-P	Max
Group delay in-band ripple	30	ns P-P	Max
Triple transit suppression	60	dB	Min

Table 14: On-board RX filter specifications.

to the linear-phase filter of the previous section. Here, A_1 is the attenuation of the useful signal (i.e. insertion loss), while $A_2 < A_1$ is the attenuation of the spurious signal. Thus the paek-to-peak ripple of the group delay amounts to

$$r_{\tau_g} = 4T_T \frac{A_2/A_1}{(1 + A_2/A_1)^2} \simeq 4T_T \frac{A_2}{A_1}. \tag{43}$$

From the specifications, we have A_2/A_1 (triple transit suppression) equal to 60 dB minimum, which means $A_2/A_1 = 10^{-3}$, and $r_{\tau_g} = 30$ ns maximum. From eqn. (43), we obtain that the transit time T_T is equal to 7.5 μs.

As for the ripple in magnitude, we have that $M(f)$ oscillates between $A_1(1 - A_2/A_1) = A_1 - A_2$ and $A_1(1 + A_2/A_1) = A_1 + A_2$. Then the ripple in the magnitude of the frequency response becomes equal to

$$20 \log_{10} \frac{A_1 + A_2}{A_1 - A_2} = \frac{20}{\log_e 10} \left(\log_e \frac{A_1 + A_2}{A_1} - \log_e \frac{A_1 - A_2}{A_1} \right) \simeq \frac{20}{\log_e 10} 2 \frac{A_2}{A_1} = 0.017 \text{ dB}$$

Figures 27 and 28 show the transfer function of the cascade of the raised cosine filter with frequency response $H(f)$ and the new filter which takes into account the group delay ripple $H_g(f)$, for the transmitter and receiver sides. Figures show $|H(f)H_g(f)|^2$, its zoom in the 1-dB bandwidth (to point out the amplitude ripple) and the group delay in the 10 dB-bandwidth. The group delay shows periodical oscillations with peak-to-valley values of 30 ns (as imposed), the peak-to-valley amplitude ripples are below 0.1 dB, the phase peak-to-valley ripples are below 0.15 degrees.

4.1 BER evaluation through the semianalytical technique

As far as the downlink channel is concerned, the presence of the filter and the nonlinear amplifier does not prevent from the use of the semianalytical technique described for the ideal transponder. For the uplink channel, on the contrary, it is necessary to measure the noise variance, which is in general different from that given in the case of ideal transponder since the RX filter modifies the power spectrum of the additive noise. The noise variance can be easily measured through simulation, and then it is sufficient to use the new noise variances in the various equations that give the error probabilities.

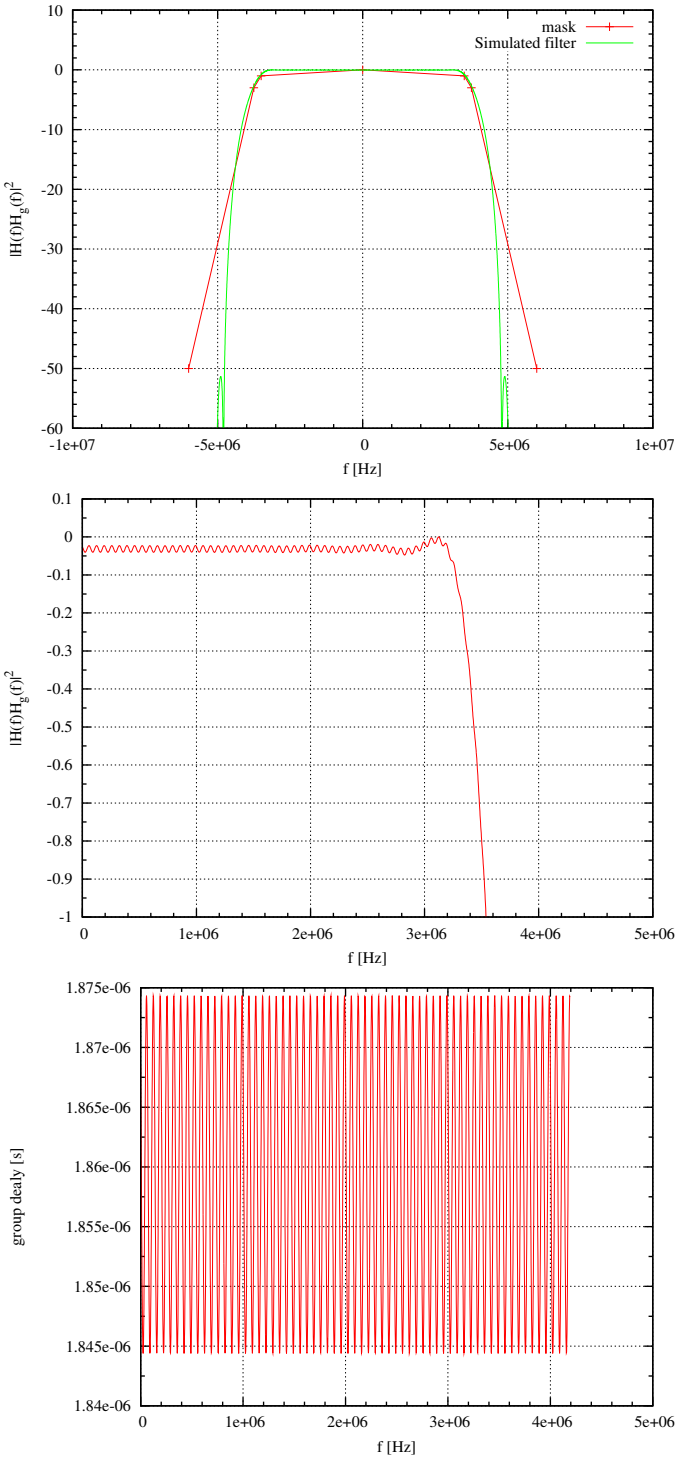

Figure 27: Transfer function for $H(f)H_g(f)$, case of transmitter filter.

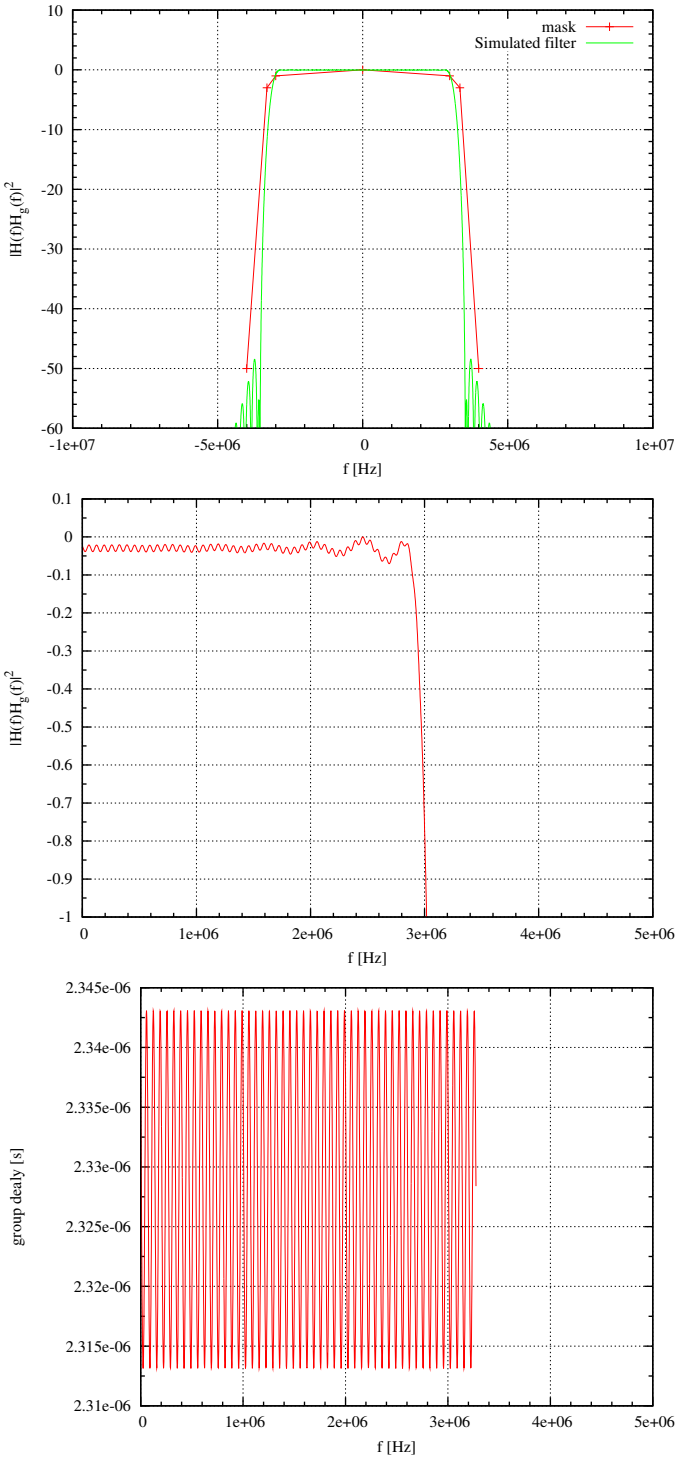

Figure 28: Transfer function for $H(f)H_g(f)$, case of receiver filter.

5 Results for the realistic transponder

5.1 Uplink with $m_{TC} = 1$ and $m_{RG} = 0.7$

The presence of the realistic transponder does not affect the performance of the telecommand system, as can be noticed from figures 29 and 30. The analysis of the performance for the ranging system is in progress.

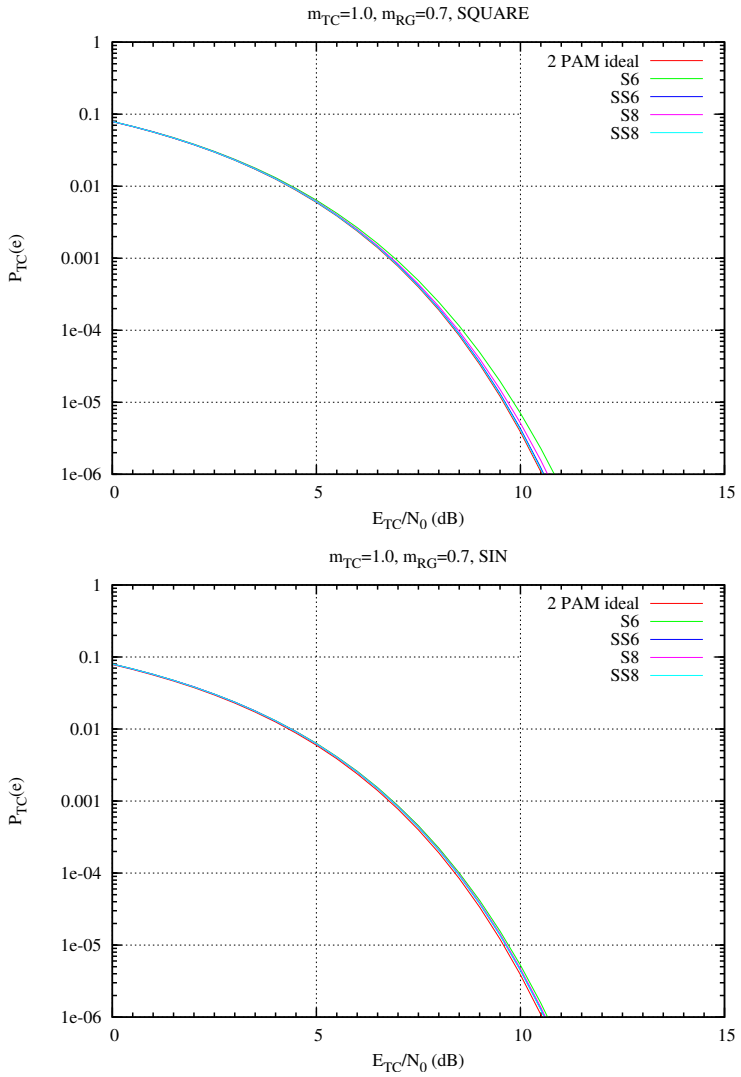

Figure 29: Error probability for telecommand with the interference of the ranging signal. Case of Stiffler codes, $h(t) = h_{sq}(t)$ (upper graph) and $h(t) = h_{sin}(t)$ (lower graph); $m_{TC} = 1$ and $m_{RG} = 0.7$, realistic transponder.

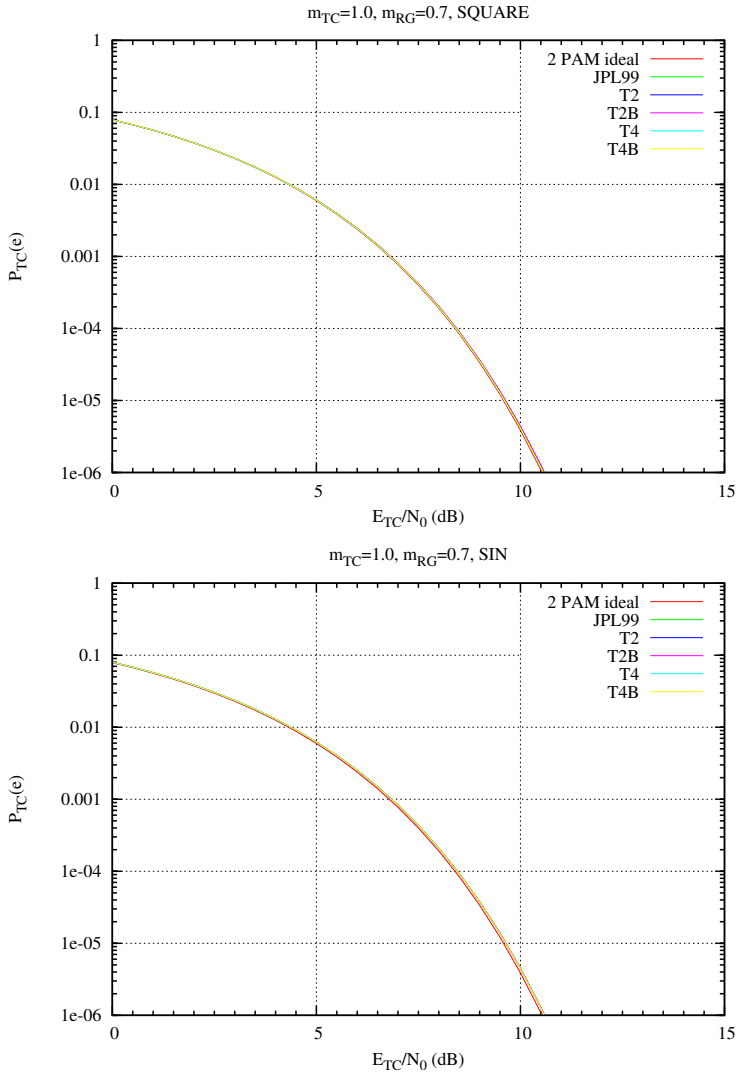

Figure 30: Error probability for telecommand with the interference of the ranging signal. Case of Tausworthe codes, $h(t) = h_{sq}(t)$ (upper graph) and $h(t) = h_{sin}(t)$ (lower graph); $m_{TC} = 1$ and $m_{RG} = 0.7$, realistic transponder.

5.2 Downlink with $m_{TM} = 1.25$ and $m_{RG} = 0.7$

The presence of the realistic transponder slightly increases the error probabilities of the telemetry system (see table 15 and figs. 31-32), but does not change the hierarchy among the various Tausworthe ranging codes: again codes T2, T2B and SS6 give the worst performance. As for the Stiffler codes, S8 shows the worst performance, while code S6 is the best.

code	$h(t) = h_{sq}(t)$	$h(t) = h_{sin}(t)$
JPL99	0.366	0.468
T2	1.193	0.713
T2B	1.182	0.706
T4	0.429	0.485
T4B	0.398	0.478
S6	0.430	0.491
SS6	0.677	0.560
S8	0.291	0.453
SS8	0.387	0.478

Table 15: Downlink losses at $P_{TM}(e) = 10^{-4}$ for the telemetry system, with the various codes; $m_{RG} = 0.7$ and $m_{TM} = 1.25$, realistic transponder.

code	$h(t) = h_{sq}(t)$	$h(t) = h_{sin}(t)$
JPL99	0.756	2.231
T2	0.223	0.284
T2B	0.300	0.280
T4	0.586	1.226
T4B	0.767	1.345
S6	0.000	0.139
SS6	0.431	0.501
S8	1.598	0.131
SS8	1.029	1.628

Table 16: Downlink losses at $P_{RG}(e) = 10^{-6}$ for the ranging system, with the various codes; $m_{RG} = 0.7$ and $m_{TM} = 1.25$, realistic transponder.

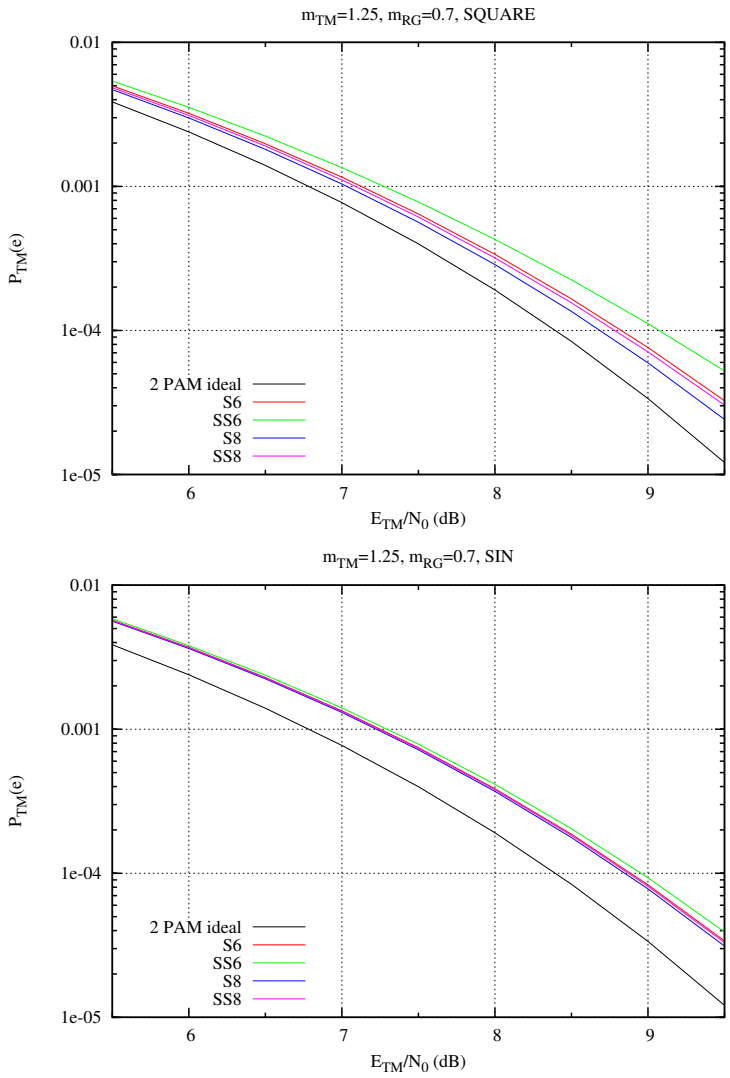

Figure 31: Error probability for telemetry with the interference of the ranging signal. Case of Stiffler codes, $h(t) = h_{sq}(t)$ (upper graph) and $h(t) = h_{sin}(t)$ (lower graph); $m_{TM} = 1.25$ and $m_{RG} = 0.7$, realistic transponder.

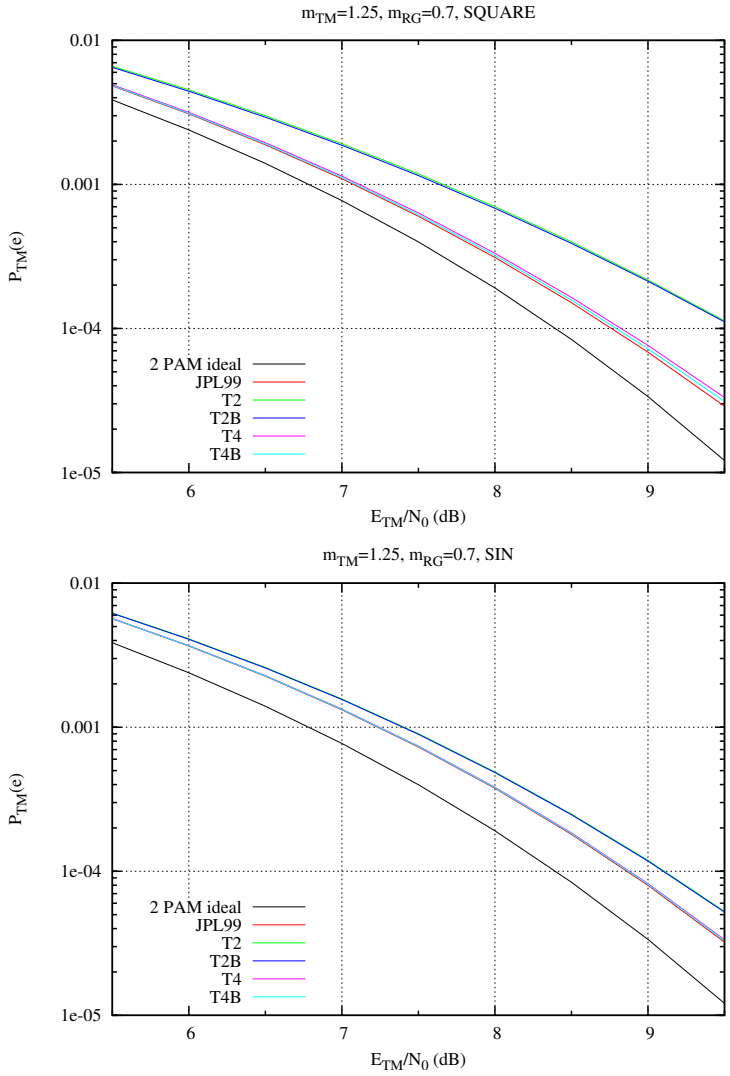

Figure 32: Error probability for telemetry with the interference of the ranging signal. Case of Tautsworth codes, $h(t) = h_{sq}(t)$ (upper graph) and $h(t) = h_{sin}(t)$ (lower graph); $m_{TM} = 1.25$ and $m_{RG} = 0.7$, realistic transponder.

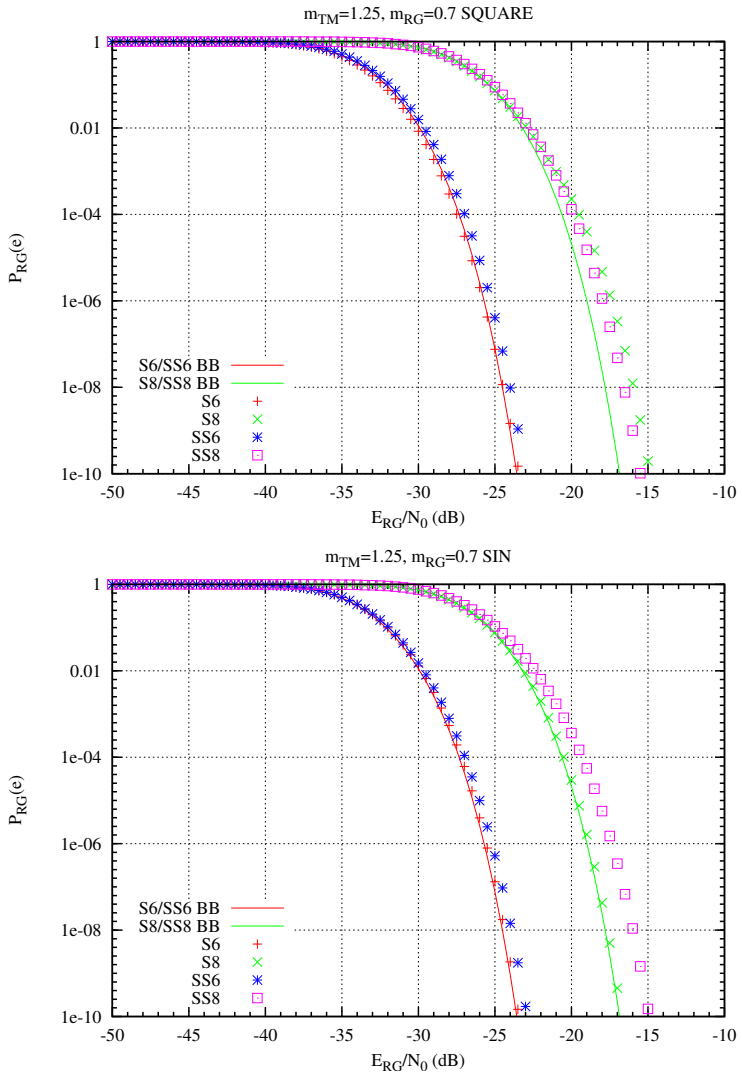

Figure 33: Error probability for the ranging system with the interference of the telemetry signal. Case of Stiffler codes observed for one ranging period, serial receiver, $h(t) = h_{sq}(t)$ (upper graph) and $h(t) = h_{sin}(t)$ (lower graph), $m_{TM} = 1.25$ and $m_{RG} = 0.7$, realistic transponder.

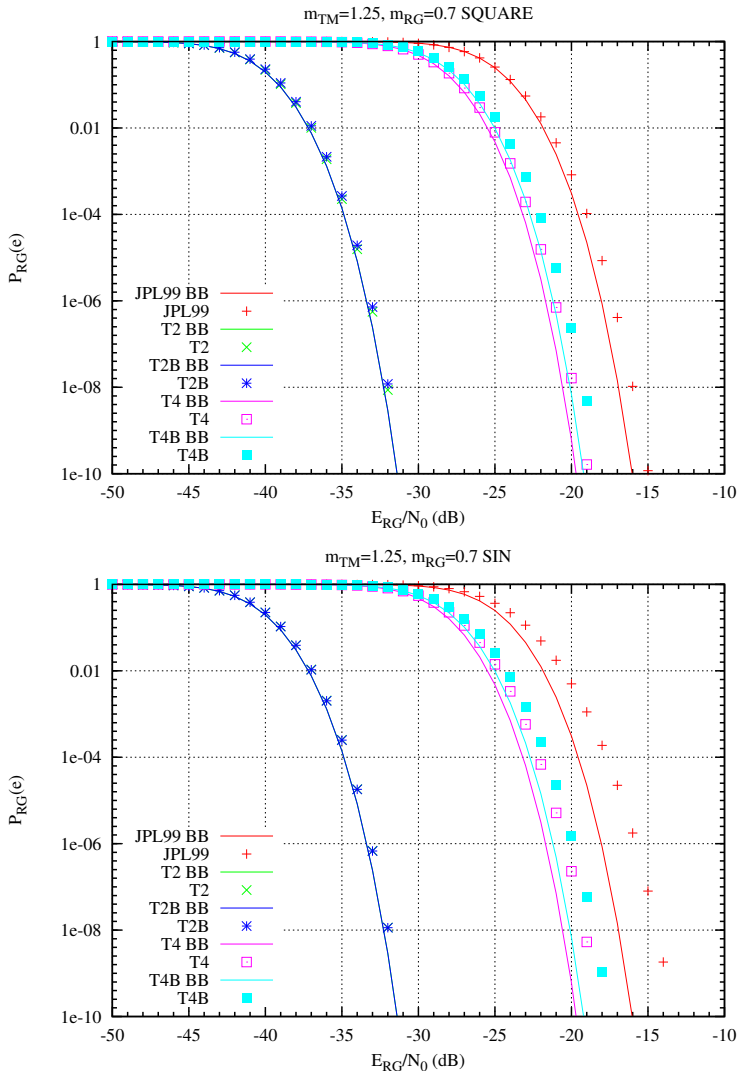

Figure 34: Error probability for the ranging system with the interference of the telemetry signal. Case of Tausworthe codes observed for one ranging period, serial receiver, $h(t) = h_{sq}(t)$ (upper graph) and $h(t) = h_{sin}(t)$ (lower graph), $m_{TM} = 1.25$ and $m_{RG} = 0.7$, realistic transponder.

5.3 Downlink with $m_{TM} = 1.25$ and $m_{RG} = 0.5$

In this case, only the error probability for the telemetry system are given to allow for comparison with the results given in [1]. The losses are given in table 17 while the error probabilities are plotted in figures 35 and 36. Codes T2 and T2B are still the worst, while the other codes are practically all equivalent. It is evident from the plots of $P_{TM}(e)$ that the realistic transponder introduces a loss of about 0.3 dB.

code	$h(t) = h_{sq}(t)$	$h(t) = h_{sin}(t)$
JPL99	0.329	0.400
T2	0.685	0.519
T2B	0.669	0.513
T4	0.351	0.407
T4B	0.338	0.404
S6	0.357	0.409
SS6	0.449	0.439
S8	0.297	0.391
SS8	0.332	0.402

Table 17: Downlink losses at $P_{TM}(e) = 10^{-4}$ for the telemetry system, with the various codes; $m_{RG} = 0.5$ and $m_{TM} = 1.25$, realistic transponder.

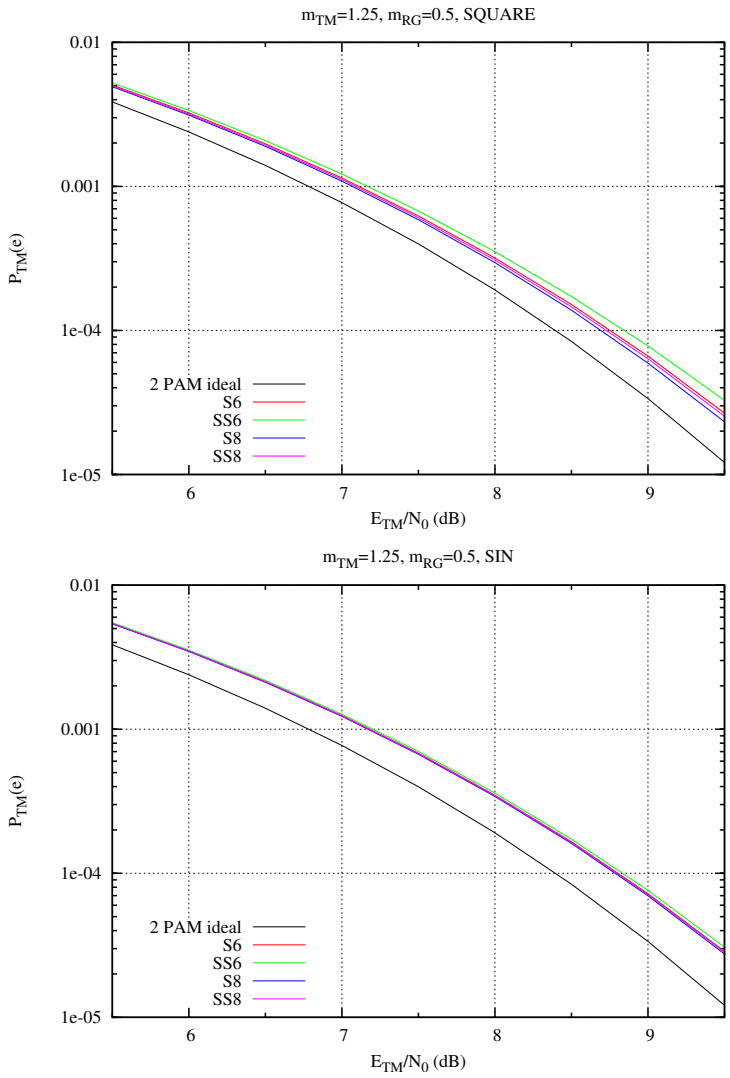

Figure 35: Error probability for telemetry with the interference of the ranging signal. Case of Stiffler codes, $h(t) = h_{sq}(t)$ (upper graph) and $h(t) = h_{sin}(t)$ (lower graph); $m_{TM} = 1.25$ and $m_{RG} = 0.5$, realistic transponder.

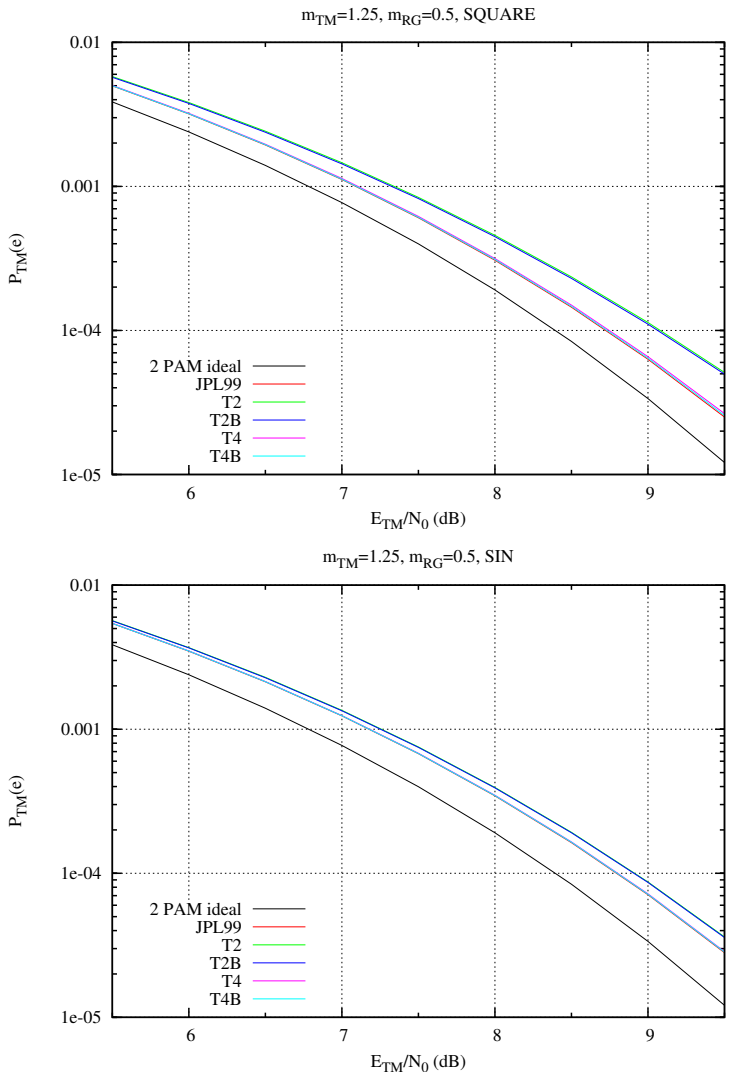

Figure 36: Error probability for telemetry with the interference of the ranging signal. Case of Tautsworth codes, $h(t) = h_{sq}(t)$ (upper graph) and $h(t) = h_{sin}(t)$ (lower graph); $m_{TM} = 1.25$ and $m_{RG} = 0.5$, realistic transponder.

5.4 Conclusions

Figures 37 and 38 show the losses for the telemetry and ranging systems for the considered codes and m_{RG} values, for the case of $h(t) = h_{sq}(t)$ and $h(t) = h_{sin}(t)$.

As for the waveform, $h_{sq}(t)$ gives now the lowest losses for both telemetry and ranging.

The hierarchy among the codes obtained from the analysis of the telemetry system is not modified by the introduction of the realistic transponder. All the losses are simply increased by a common term equal to approximately 0.3 dB due to intersymbol interference.

When considering the losses of the ranging system, we see that the realistic transponder only slightly increases the losses with respect to the ideal one for $h(t) = h_{sin}(t)$ (the added loss is about 0.1-0.2 dB). The use of $h_{sq}(t)$ together with the realistic transponder seems to negatively affect the performance of codes SS6 and SS8, for which the detector takes the wrong decision even in the absence of noise; on the contrary, code S8 seems to have larger losses for larger values of m_{RG}, which is not justifiable. A deeper analysis showed that the nonlinear TWTA actually amplifies the dependency of the Stiffler ranging system performance on the telemetry bit sequence, so that the obtained losses cannot be considered reliable for any of the Stiffler codes.

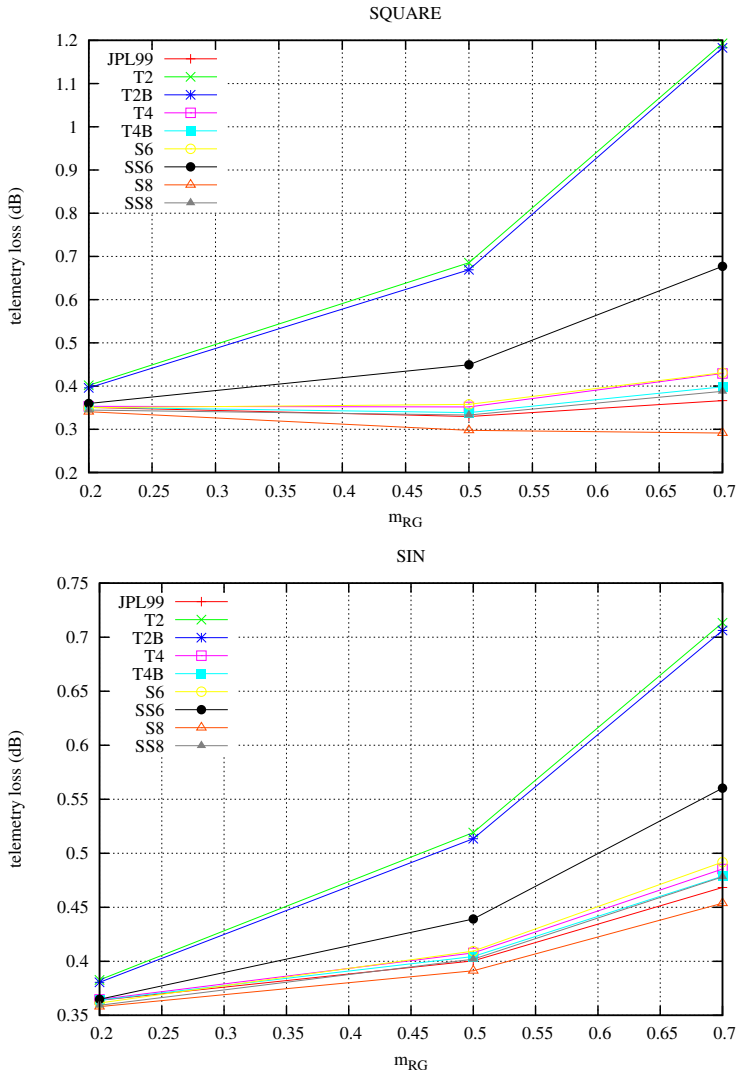

Figure 37: Losses for the telemetry system at $P_{TM}(e) = 10^{-4}$ as function of m_{RG} for the various codes, $h(t) = h_{sq}(t)$ (upper graph) and $h(t) = h_{sin}(t)$ (lower graph), $m_{TM} = 1.25$ realistic transponder.

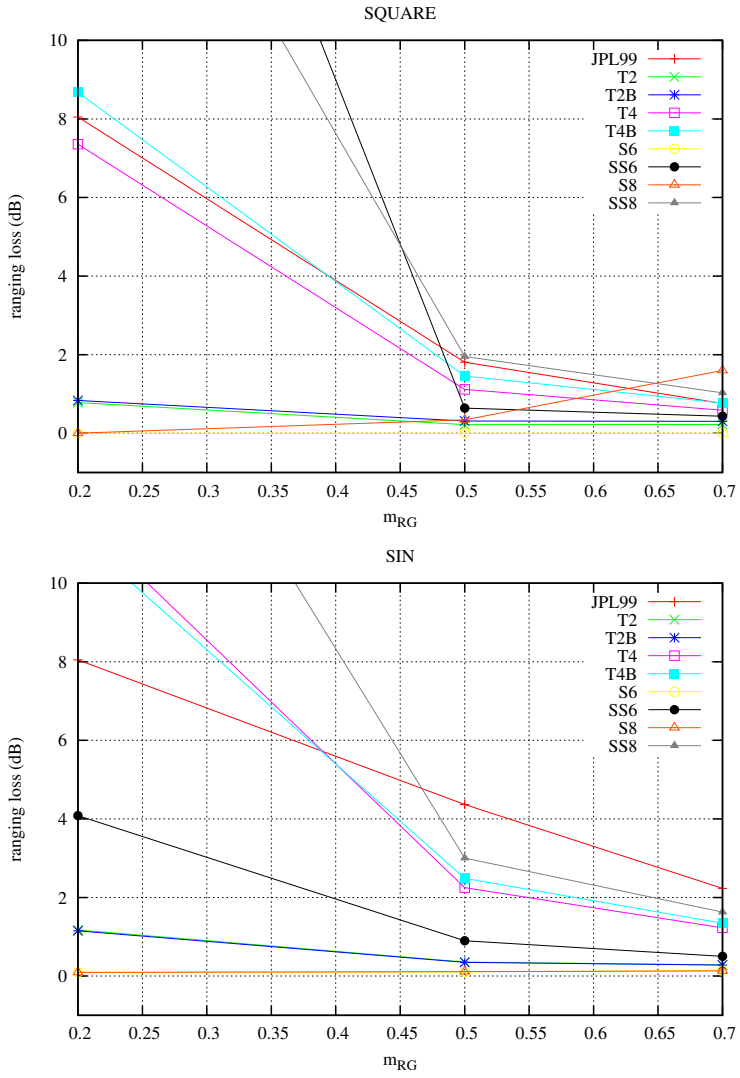

Figure 38: Losses for the ranging system at $P_{RG}(e) = 10^{-6}$ as function of m_{RG} for the various codes, $h(t) = h_{sq}(t)$ (upper graph) and $h(t) = h_{sin}(t)$ (lower graph), $m_{TM} = 1.25$ realistic transponder.

References

[1] G. Boscagli, P. Holsters, *AI_04-08: Analyze the RFI of all proposed PN Ranging Schemes with TC/TM*, CCSDS Fall Meeting, Darmstadt, November 2005, SLS-RNG_05-04

[2] Gradshteyn, Ryzhik, *Tables of integrals, series and products*, Academic Press, 5-th ed., 1994.